EPRI | ELECTRIC POWER RESEARCH INSTITUTE

Steam Generator Management Program: Flaw Tolerance Evaluation of the Steam Generator Channel Head

2013 TECHNICAL REPORT

Steam Generator Management Program: Flaw Tolerance Evaluation of the Steam Generator Channel Head

3002000411

Final Report, April 2013

EPRI Project Manager
H. Cothron

ELECTRIC POWER RESEARCH INSTITUTE
3420 Hillview Avenue, Palo Alto, California 94304-1338 ▪ PO Box 10412, Palo Alto, California 94303-0813 ▪ USA
800.313.3774 ▪ 650.855.2121 ▪ askepri@epri.com ▪ www.epri.com

DISCLAIMER OF WARRANTIES AND LIMITATION OF LIABILITIES

THE FOLLOWING ORGANIZATION, UNDER CONTRACT TO EPRI, PREPARED THIS REPORT:

Structural Integrity Associates, Inc.

THE TECHNICAL CONTENTS OF THIS DOCUMENT WERE PREPARED IN ACCORDANCE WITH THE EPRI NUCLEAR QUALITY ASSURANCE PROGRAM MANUAL THAT FULFILLS THE REQUIREMENTS OF 10 CFR 50 APPENDIX B, 10 CFR PART 21, ANSI N45.2-1977 AND/ OR THE INTENT OF ISO-9001 (1994). CERTIFICATION OF CONFORMANCE CAN BE OBTAINED FROM EPRI. BEFORE THE CONTENTS OF THIS DOCUMENT CAN BE APPLIED TO FULFILL QUALITY PROGRAM REQUIREMENTS, CONTRACTUAL ARRANGEMENTS BETWEEN THE USER AND EPRI MUST BE ESTABLISHED. USE OF THE CONTENTS OF THIS DOCUMENT IN NUCLEAR SAFETY OR NUCLEAR QUALITY APPLICATIONS MAY ALSO REQUIRE FURTHER ACCEPTANCE REVIEWS/ACTIONS PURSUANT TO USER'S INTERNAL PROCEDURES.

NOTE

For further information about EPRI, call the EPRI Customer Assistance Center at 800.313.3774 or e-mail askepri@epri.com.

ACKNOWLEDGMENTS

The following organization, under contract to the Electric Power Research Institute (EPRI), prepared this report:

Structural Integrity Associates, Inc.
11515 Vanstory Drive, Suite 125
Huntersville, NC 28078

Principal Investigators
C. Fourcade
A. Miessi

This report describes research sponsored by EPRI.

This publication is a corporate document that should be cited in the literature in the following manner:

Steam Generator Management Program: Flaw Tolerance Evaluation of the Steam Generator Channel Head. EPRI, Palo Alto, CA: 2013. 3002000411.

PRODUCT DESCRIPTION

Indications have previously been reported in the steam generator divider plate at operating plants outside the United States. The function of the divider plate in most steam generators is to separate the cold and hot legs of the channel head as the primary water enters the steam generator so that the primary coolant flows up into the tubes. As such, the divider plate is not considered a primary pressure boundary component or a structural component of the lower steam generator complex. However, the propagation of cracks into the steam generator channel head is a concern.

There are two cracking scenarios of concern: cracks propagating from the divider plate assembly through the channel head cladding and into the low-alloy steel, and cracks initiating in the tubesheet and propagating through the tube-to-tubesheet weldments. Both scenarios represent a potential breach of the primary pressure boundary of the channel head assembly. This report addresses only the first cracking scenario and its potential impact on the structural integrity of the steam generator channel head.

Background

The divider plate cracks have been attributed to material defects, weld defects, damage due to foreign objects in the channel head, and primary water stress corrosion cracking. Industry operating experience and nondestructive examinations of the reported indications have shown that, although they could run nearly the length of the divider plate, the cracks remain shallow, in many cases less than one-tenth of the divider plate thickness.

In a previous Electric Power Research Institute (EPRI) report (1014982), the effects of a crack in the divider plate on the structural integrity of the lower steam generator complex was evaluated. Report 1014982 concluded that the cracks reported in the foreign steam generators could not cause failure of the divider plate in the limiting domestic steam generators during the design basis accident or normal operating conditions. However, it was shown that cracks in the divider plate–to–stub runner weld could grow in both length and depth.

Objective

The purpose of this report is to document the evaluation of the impact of a flaw from a cracked divider plate propagating into the steam generator channel head. The report summarizes the stress and fracture mechanics analyses performed to assess the flaw tolerance of the steam generator channel head.

Approach

Detailed three-dimensional finite element stress analyses were performed to determine the critical stresses in the steam generator channel head assembly. The bounding stresses at the critical locations of the channel head were input to a fatigue crack growth analysis. Fracture mechanics analyses were performed to determine the flaw tolerance of the steam generator channel head.

Results

The flaw tolerance evaluation demonstrated that the structural integrity of the steam generator channel head was not compromised by a crack in the divider plate. Assumed axial and circumferential flaws in the steam generator channel head material remained well below the allowable flaw depths after 40 years of operation. The evaluation included several design input assumptions based on industry data or engineering judgment, both of which are generally conservative.

Application, Value, and Use

Utilities can use the results from this analysis to determine the need to inspect steam generator Alloy 600 material in the divider plate assembly or the low-alloy steel channel head material in the period of operation beyond 40 years. Utilities can use this information to update their Aging Management Program developed during the plant life extension approval process.

Keywords

Divider plate
Fatigue crack growth
Steam generator channel head
Tubesheet

CONTENTS

LIST OF FIGURES

LIST OF TABLES

1
INTRODUCTION

There have been several documented cases of crack indications in the divider plate assembly in Westinghouse model steam generators in operation outside of the United States. The region of cracking concern is shown in Figure 1-1. These indications were observed in plants that operated with proper primary water chemistry. The function of the divider plate in most steam generators is to separate the cold and hot legs of the channel head as the primary water enters the steam generator so that the primary coolant flows up into the tubes. The divider plate is not generally considered a primary pressure boundary component or a structural component of the lower steam generator complex. It should be noted that recently designed replacement steam generator models do include the divider plate as a required structural component in the lower steam generator complex. These steam generators are in the minority in the domestic fleet. Nevertheless, the flaw tolerance evaluation presented in this report takes into account the structural response of the divider plate. Hence, the evaluation is applicable to all steam generator channel heads with a divider plate considered in this study, including those for which the divider plate is treated as a structural member.

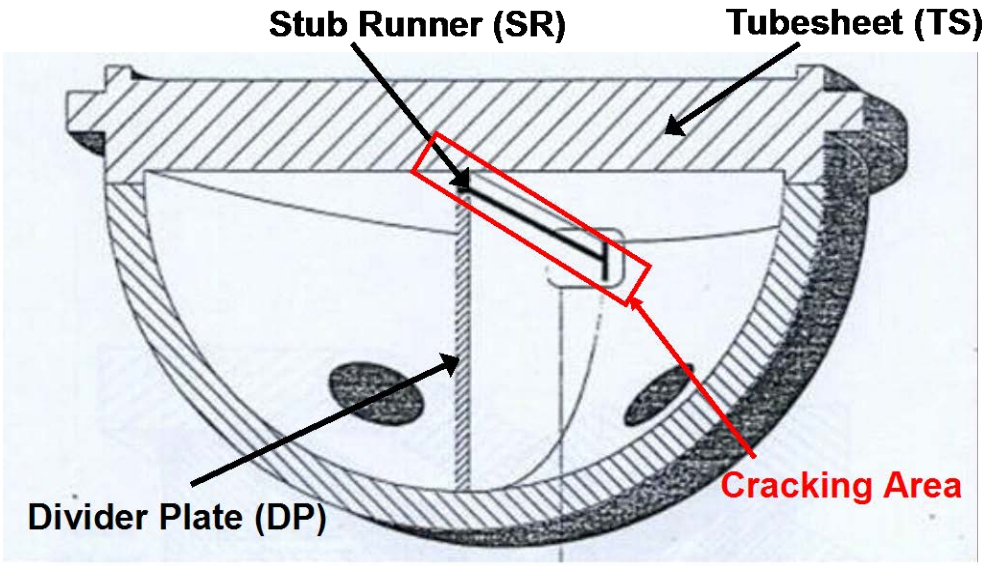

Figure 1-1
Schematic of Channel Head Assembly and Reported Cracking Locations

In most Model F, Model D and Model 51 Westinghouse pressurized water reactor (PWR) steam generators the divider plate is initially welded to the post-clad channel head and then attached to the tubesheet via a weld to a strip of metal on the primary face of the tubesheet called the stub runner (Figure 1-2). The weld between the stub runner and the divider plate is subject to bending and tensile stresses (e.g., membrane and bending) during regular operation of the steam

generator. The membrane stresses on the divider plate occur as the tubesheet bows from the difference between the primary and secondary operating pressures. Bending of the divider plate occurs because there typically is a temperature and a pressure difference between the hot leg and cold leg side of the tubesheet and divider plate. The full penetration weld that joins the stub runner and the divider plate in some steam generators applies Filler Metal (FM) 82 bare wire or rod or FM182 coated electrodes depending on the welding process applied. In most cases both filler materials will be used in the same weld depending on the process used – gas tungsten arc welding (GTAW) or gas metal arc welding (GMAW) versus shielded metal arc welding (SMAW).

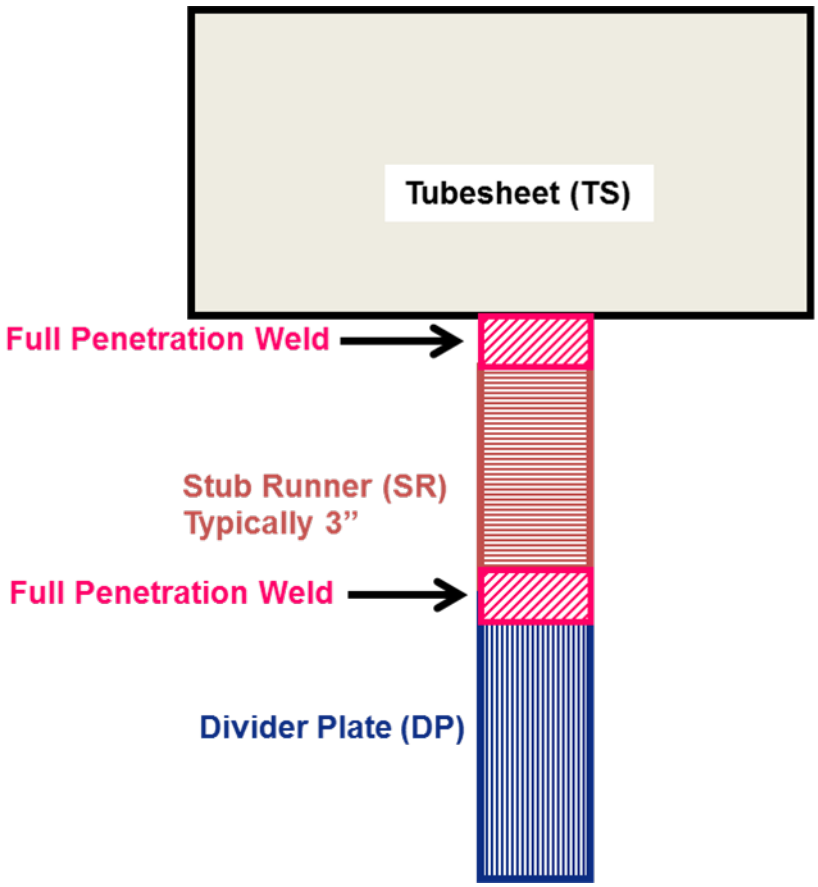

Figure 1-2
Schematic Cross-section of Tubesheet to Divider Plate Welds

In 2010, the Steam Generator Management Program completed an investigation on the safety significance of the reported divider plate crack indications and the need for US plants to begin inspections. Research evaluated a bounding crack opening area for transient analyses, LOCA and non-LOCA analyses, ASME Stress Report fatigue limits, alternate repair criteria, and installed plugs and sleeves. The investigation concluded that a crack running the full length and depth of the weld is not a safety concern, thus expanded inspection protocols for the US fleet are not warranted. It is important to note that no suitable inspection techniques are qualified in the US for performing these inspections. In addition, the inspections that have been performed in the non-US plants were reported to be time-consuming and dose intensive.

As US plants began entering into the period of extended operation through license renewal, the NRC asked for the inventory of Alloy 600 in the steam generator. It was postulated that primary water stress corrosion cracks (PWSCC) that might initiate in an Alloy 600 divider plate/stub runner or in the FM 82/182 welds that join them could propagate over time to pressure boundaries such as the tube-to-tubesheet weld or perhaps into the channel head wall itself. The former scenario might eventually result in a primary-to-secondary leak, and the latter might lead to a breach of the primary pressure boundary itself. Both postulated scenarios are under consideration as part of aging management programs (AMPs); however, it is important to note that no documented operational experience to date supports either scenario.

In the latter scenario, PWSCC initiation might occur within the divider plate assembly (Alloy 600) and could follow a path that conceivably could reach the channel head, which is a primary pressure boundary. The channel head is carbon steel and is not susceptible to PWSCC. However, the stress state in this region is not completely defined and might be sufficient to result in further crack extension via mechanical fatigue. This scenario is applicable to U.S. (30 units) and non-U.S. steam generators. The Steam Generator Management Project (SGMP) began a three-year project in 2011 to investigate the likelihood that cracks might initiate and propagate as proposed by the NRC.

This report summarizes an evaluation of the flaw tolerance of the steam generator channel head, should a divider plate crack reach the channel head wall. Detailed finite element stress analyses are performed to determine the critical stresses in the channel head complex and fracture mechanics evaluations, including fatigue crack growth analyses, are conducted to determine how much an axial flaw or a circumferential flaw would propagate in the channel head and whether the crack growth would remain below ASME Code Section XI limits [2].

2
FINITE ELEMENT ANALYSES

Detailed three-dimensional (3D) finite element stress analyses were performed to determine the critical stresses in the steam generator channel head assembly. The bounding stresses at the critical locations of the channel head were input to the fatigue crack growth analysis described in Section 3.

Finite Element Model

A 3D finite element model of the steam generator channel head assembly is developed and used to analyze internal pressure loading and thermal transient conditions. The finite element model, which is constructed using the ANSYS finite element software [3], includes the steam generator bottom channel head, the divider plate, stub runner, tubesheet, and associated welds. The model also includes the stainless steel channel head cladding and Alloy 82/182 tubesheet cladding.

The general dimensions of the channel head assembly are taken from Reference 1 which determined that, for the divider plate cracking issue, the most limiting steam generator model is the Westinghouse Model 51 steam generator. The principal dimensions used are shown in Figure 2-1. Whenever specific dimensions were not explicitly listed in Reference 1, values were assumed based on technical industry data. Plots of the finite element model are shown in Figure 2-2.

For the purpose of this flaw tolerance evaluation, a planar through-wall crack is postulated in the divider plate PWSCC susceptible weld. Thus, a flaw is introduced in the finite element model at the interface between the divider plate and tubesheet, starting at the steam generator wall (triple-point), and extending horizontally approximately one-quarter of the steam generator radius. The modeled crack is about 15 inches in length, which is approximately 8 times the thickness of the divider plate. The modeled flaw is illustrated in the exaggerated crack opening displaced shape plot shown in Figure 2-9.

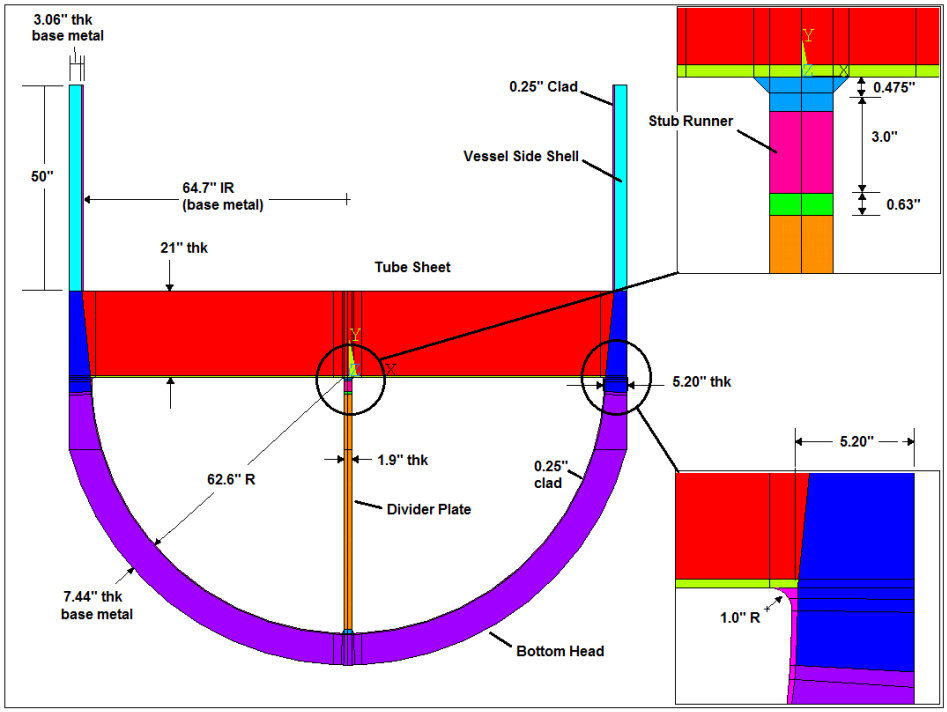

Figure 2-1
Channel Head Assembly Dimensions

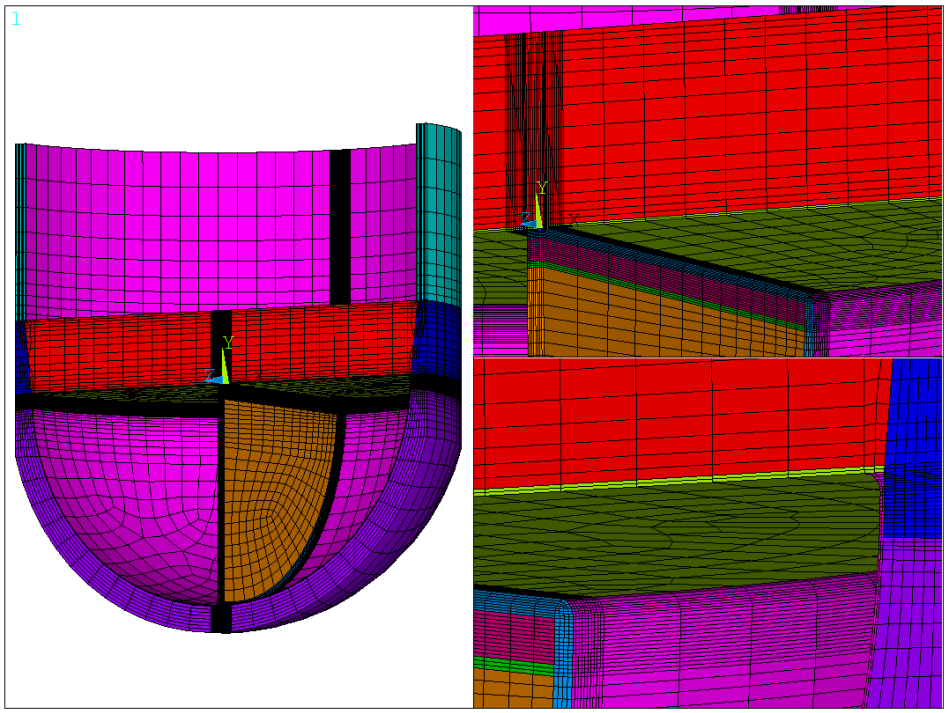

Figure 2-2
3D Finite Element Model Mesh

Materials of SG Channel Head Assembly

The materials of the different components of the limiting Westinghouse Model 51 steam generator channel head assembly are listed in Reference 1. The material specifications are tabulated in Table 2-1. The material of the cladding on both the bottom head and steam generator vessel is assumed to be Type 309L whereas the tubesheet cladding and the stub runner-to-tubesheet fillet weld are assumed to be Inconel ERNiCr-3. The cladding and fillet weld are assigned equivalent base metal properties in the finite element analyses. The temperature-dependent material properties for each of the components of the channel head assembly are obtained from the ASME Boiler and Pressure Vessel Code, Section II, Part D [2].

Table 2-1
Material Specification

Component	Material	References
Steam Generator Bottom Head	SA-216 WCC	[1]
Bottom Head Cladding and Vessel Cladding	Type 309L Stainless Steel Treated as Type 304 SS	Assumed
Vessel Side Shell	SA-533 Grade A, Class 1	[1]
Tubesheet	SA-508, Class 2	[1]
Tubesheet Cladding	Inconel ERNiCr-3 Treated as Alloy 82/182	Assumed
Stub Runner	Alloy 600	[1]
Divider Plate	Alloy 600	[1]
Stub Runner-to-Divider Weld	Inconel ERNiCr-3 Treated as Alloy 82/182	[1]
Stub Runner-to-Tubesheet Fillet Weld	Inconel ERNiCr-3 Treated as Alloy 82/182	Assumed

Applied Loads and Boundary Conditions

The steam generator channel head is subjected to different internal pressure levels and thermal transients during its design life. The specified design basis plant conditions for the limiting steam generator are used in the flaw tolerance evaluation.

Internal Pressure

The operating pressures given in the Reference 1 report are applied to the separate chambers of the steam generator. The hot leg side is given as 2250 psi, the cold leg side is 2200 psi, and the upper (secondary) side above the tube sheet is 735 psi [1]. Crack face pressure of 2250 psi is also applied to the surfaces of the modeled crack at the divider plate/tubesheet interface.

The applied pressure is shown in Figure 2-3. The nodes at the top free end are fixed in the axial direction and symmetry boundary conditions are applied at the plane of symmetry, as shown in Figure 2-4.

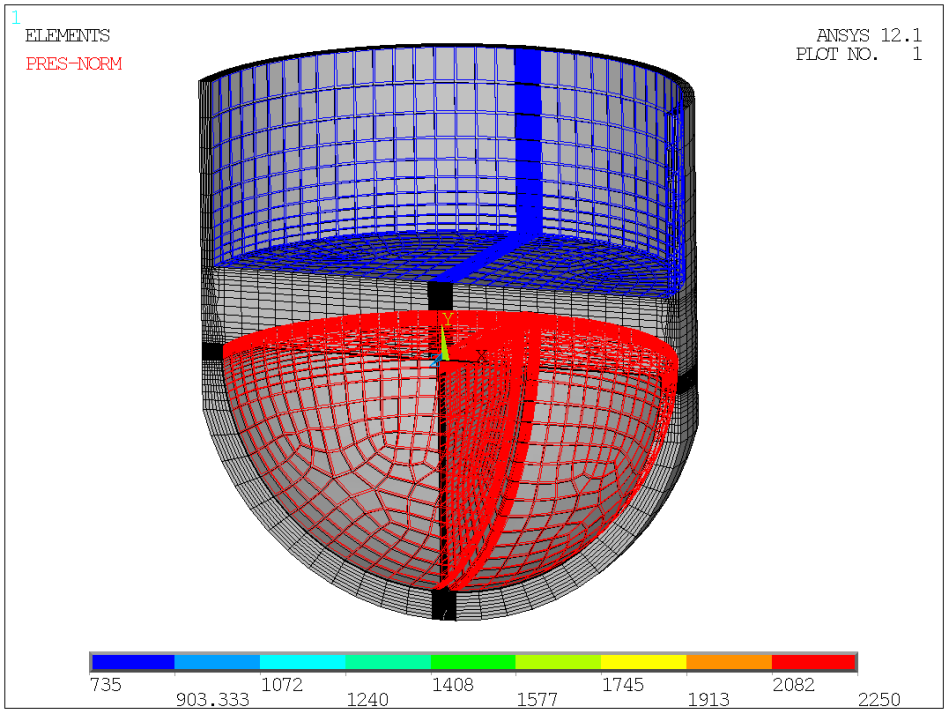

Figure 2-3
Internal Pressure Loading

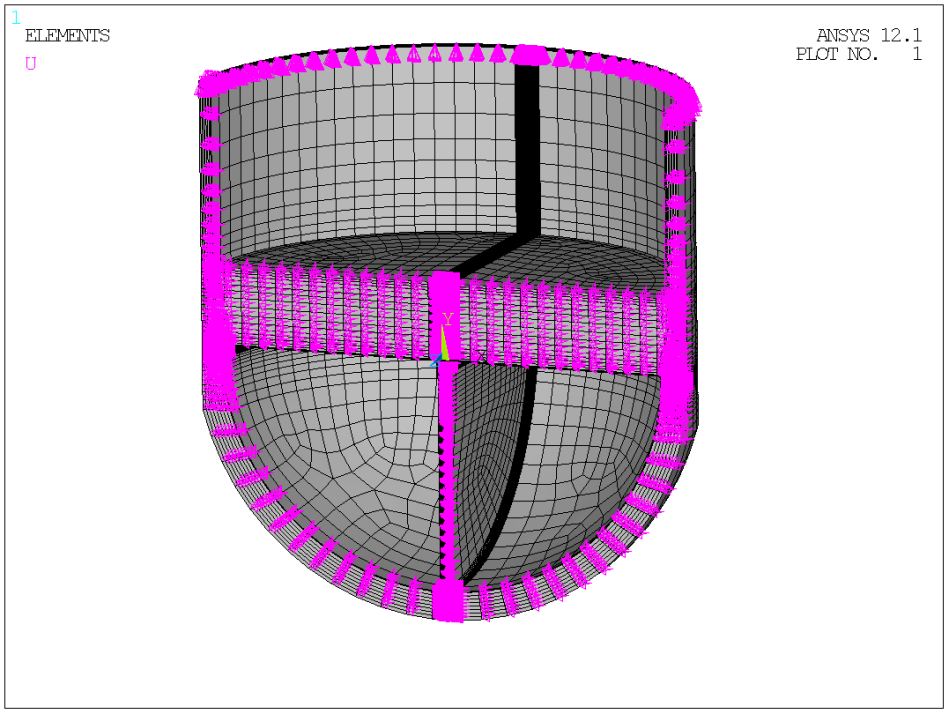

Figure 2-4
Structural Boundary Conditions

Thermal Transients

The thermal transients were developed for the steam generator hot leg and cold leg side for the design basis plant conditions. The bounding thermal transients analyzed for this evaluation are listed in Table 2-2 and Table 2-3 for the hot leg and cold leg sides of the channel head, respectively. Thirteen separate thermal transients are evaluated along with a separate unit internal pressure evaluation, and a separate analysis is performed to capture the hydro/leak test thermal stress states.

For each thermal transient, heat transfer coefficients for forced flow were calculated based on typical PWR hot leg and cold leg fluid conditions and flow rates at each time point in Table 2-2 and Table 2-3, and equations from Reference 9. Bulk fluid temperatures and heat transfer coefficients are applied to the interior surface nodes of the model as provided in Table 2-2 and Table 2-3. In addition, separate bulk temperature and heat transfer coefficients are applied to the upper chamber (secondary side) above the tubesheet as follows:

- For the normal operating transients (heatup, cooldown, load, unload, step increase/decrease, feedwater cycling), a saturated temperature of 509°F (corresponding to the secondary pressure of 735 psi [1]), and assumed stagnant natural circulation heat transfer coefficient of h = 100 Btu/hr-ft²-°F is applied.
- For the Upset transients (loss of load, loss of power, loss of flow, reactor trip, turbine roll test, hydro/leak tests), a slightly lower pressure of 695 psi is assumed, and corresponding bulk fluid temperature of 502°F is applied.

Figure 2-5 shows a representative plot of the applied heat transfer coefficients for one of the thermal transient analyses (Plant Cooldown). The heat transfer coefficient is a fundamental measurement of convective heat transfer that occurs between a surface and a moving fluid when they are at different temperatures.

Previous analyses have shown that, due to the thermal interaction of the tubes and the tubesheet, the tubesheet remains essentially isothermal during the thermal transients of the steam generator channel head [8]. Consequently, vertical through-thickness thermal gradients are seen only in the top 2-inch layer of the tubesheet. A thermal degree-of-freedom coupling scheme is used to simulate this boundary condition in the finite element analyses.

Symmetry boundary conditions are applied at the planes of symmetry, as shown in Figure 2-4. The reference temperature for the thermal stress calculation is assumed to be 70°F.

Table 2-2
Bounding Thermal Transients – Hot Leg Side

Description	Time, sec	T, °F	P, psia	Cycles	h, Btu/hr-ft²-°F
Plant Heatup	0	70	400	200	2885.3
	17172	547	2250		6132.7
Plant Cooldown	0	547	2250	200	6132.7
	17172	70	400		2885.3
Plant Loading	0	547	2250	18300	6132.7
	1200	621.9	2250		6024.0
Plant Unloading	0	621.9	2250	18300	6024.0
	1200	547	2250		6132.7
Small Step Load Increase	0	621.9	2250	2000	6024.0
	50	616.9	2185		6019.8
	180	625.9	2315		6024.0
	300	629.9	2280		6024.0
Small Step Load Decrease	0	621.9	2250	2000	6024.0
	30	626.9	2325		6024.0
	150	619.9	2175		6019.8
	300	613.9	2240		5991.1
Large Step Load Decrease	0	621.9	2250	200	6024.0
	60	626.9	2350		6033.3
	480	578.9	1975		6062.0
	1200	542.9	2210		6146.1
Feedwater Cycling @ Hot Standby	0	621.9	2250	25000	6024.0
	720	594.9	2225		5991.8
	3960	626.9	2280		6024.0
	4500	621.9	2250		6024.0
Loss of Load	0	621.9	2250	80	6024.0
	26	647.9	2550		6053.5
	60	583.9	1710		6062.0
	100	558.9	1600		6093.9
Loss of Power	0	621.9	2250	40	6024.0
	129	597.9	2070		1653.4
	2700	641.9	2500		366.2
	9720	602.9	2300		361.0
Loss of Flow	0	621.9	2250	80	6024.0
	15	627.9	2220		6024.0
	25	551.9	2100		6116.7
	50	506.9	1950		6263.3
	140	525.9	1875		6201.4
Reactor Trip	0	621.9	2250	400	6024.0
	20	566.9	1980		6067.9
	40	549.9	1890		6132.7
	100	543.9	1870		6146.1

Table 2-2 (continued)
Bounding Thermal Transients – Hot Leg Side

Description	Time, sec	T, °F	P, psia	Cycles	h, Btu/hr-ft²-°F
Turbine Roll Test	0	547	2250	10	6132.7
	1680	475	1920		6181.1
Primary Side Hydro Test (Shop)*		70	15	5	NA
		250	3122		
		70	15		
Primary Side Hydro Test (Field)*		400	2250	50	NA
		547	2500		
		400	2250		
Primary-to-Secondary Leak Test*		70	15	90	NA
		547	2265		
		70	15		

* It is assumed that each hydro/leak test includes a heatup/pressurization, a steady state and then a cooldown/depressurization. The heatup/cooldown rate is assumed to be slow enough so as to not create transient thermal stresses, only steady-state stresses. Therefore, only the initial, steady state and end conditions are listed, and no heat transfer coefficients need be applied.

Table 2-3
Bounding Thermal Transients – Cold Leg Side

Description	Time, sec	T, °F	P, psia	Cycles	h, Btu/hr-ft²-°F
Plant Heatup	0	70	400	200	2885.3
	17172	547	2250		6132.7
Plant Cooldown	0	547	2250	200	6132.7
	17172	70	400		2885.3
Plant Loading	0	547	2250	18300	6132.7
	1200	552	2250		6119.7
Plant Unloading	0	552	2250	18300	6119.7
	1200	547	2250		6132.7
Small Step Load Increase	0	552	2250	2000	6119.7
	60	539	2185		6181.6
	180	550	2315		6132.7
	300	554	2280		6119.7
Small Step Load Decrease	0	552	2250	2000	6119.7
	50	567	2325		6070.8
	150	557	2175		6100.1
	300	551	2240		6119.7

Table 2-3 (continued)
Bounding Thermal Transients – Cold Leg Side

Description	Time, sec	T, °F	P, psia	Cycles	h, Btu/hr-ft²-°F
Small Step Load Decrease	0	552	2250	2000	6119.7
	50	567	2325		6070.8
	150	557	2175		6100.1
	300	551	2240		6119.7
Large Step Load Decrease	0	552	2250	200	6119.7
	60	567	2350		6070.8
	480	555	1975		6119.7
	1200	542	2210		6149.0
Feedwater Cycling @ Hot Standby	0	552	2250	25000	6119.7
	720	525	2225		6204.4
	3960	557	2280		6100.1
	4500	552	2250		6119.7
Loss of Load	0	552	2250	80	6119.7
	30	587	2550		6046.1
	60	566	1710		6070.8
	100	555	1600		6119.7
Loss of Power	0	552	2250	40	6119.7
	129	562	2070		1678.8
	720	551	2500		370.2
	9720	551	2300		370.2
Loss of Flow	0	552	2250	80	6119.7
	15	507	2220		6263.0
	25	532	2100		6181.6
	45	552	1950		6119.7
	140	540	1875		6181.6
Reactor Trip	0	552	2250	400	6119.7
	20	545	1980		6149.0
	40	542	1890		6149.0
	100	542	1870		6149.0

Table 2-3 (continued)
Bounding Thermal Transients – Cold Leg Side

Description	Time, sec	T, °F	P, psia	Cycles	h, Btu/hr-ft²-°F
	0	547	2250	10	6132.7
Turbine Roll Test	1680	475	1920		6182.7
		70	15	5	NA
		250	3122		
Primary Side Hydro Test (Shop)*		70	15		
		400	2250	50	NA
		547	2500		
Primary Side Hydro Test (Field)*		400	2250		
		70	15	90	NA
		547	2265		
Primary-to-Secondary Leak Test*		70	15		

* It is assumed that each hydro/leak test includes a heatup/pressurization, a steady state and then a cooldown/depressurization. The heatup/cooldown rate is assumed to be slow enough so as to not create transient thermal stresses, only steady-state stresses. Therefore, only the initial, steady state and end conditions are listed, and no heat transfer coefficients need be applied.

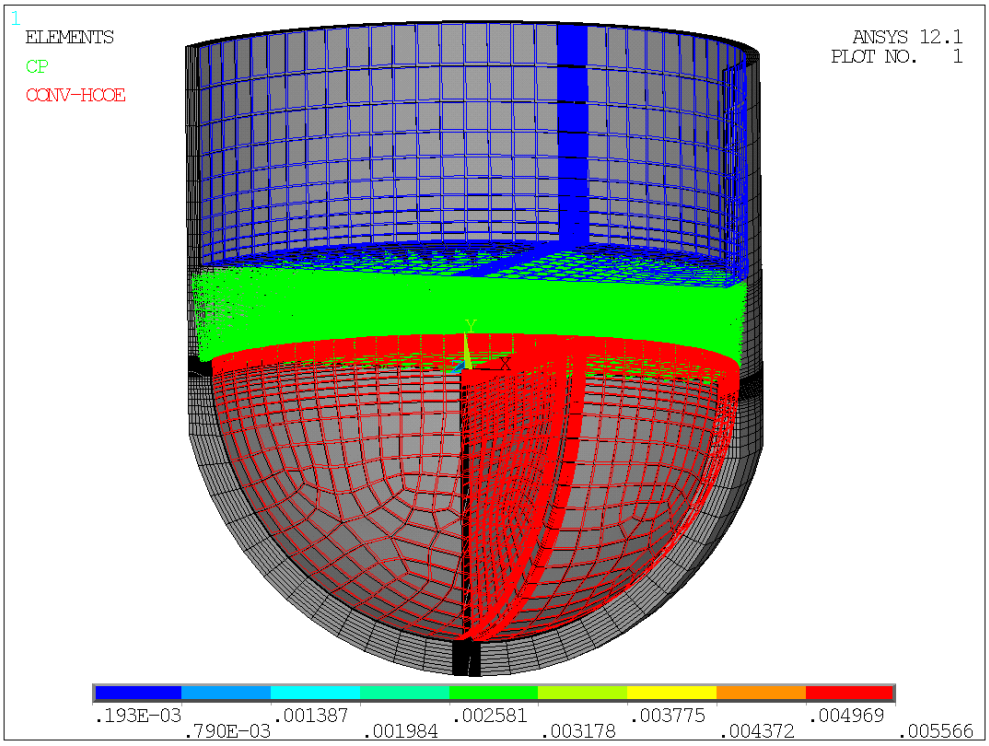

Figure 2-5
Representative Thermal Boundary Conditions. Units shown for heat transfer coefficients are Btu/sec-in^2-°F.

Finite Element Stress Analysis Results

The results of the finite element stress analyses are post-processed for use in the fracture mechanics analyses described in Section 3. A sample resulting temperature distribution in the channel head assembly is presented in Figure 2-6 and a sample stress plot is shown in Figure 2-7 for the Plant Cooldown transient.

Several through-wall stress paths are defined through the weld attachment region between the stub runner, tubesheet, and channel head wall (referred to herein as the “triple-point” location), and both hoop and axial stresses are extracted along these paths. The paths are chosen based on the locations that have stress concentrations, which are typically at either side of the weld. The stress path locations are shown in Figure 2-8.

The flaws postulated herein were not physically modeled in the finite element stress analyses. Rather, the stress components that act perpendicular to the crack face of the postulated flaws are used with standard fracture mechanics models. Therefore, the axial stresses are used for the postulated circumferential flaws, and the hoop stresses are used for the postulated axial flaws. The stresses are selected at the times of maximum and minimum inside surface linearized membrane-plus-bending stress states.

Based on a review of each stress path, Path 1, Path 2, and Path 3 are determined to produce the bounding stress results. Therefore, the through-wall hoop and axial stresses at those critical paths are extracted for use in the fracture mechanics evaluation described in Section 3. The maximum and minimum hoop stress distributions are plotted in Figure 2-10, Figure 2-11 and Figure 2-12. Likewise, the maximum and minimum axial stress distributions are plotted in Figure 2-13, Figure 2-14 and Figure 2-15.

In addition to the thermal and pressure stress, weld residual stresses are considered in the analyses, since the proximity of the channel head seam welds with respect to the triple point flaw location is unknown. The through-wall weld residual stress profile, which is prescribed for post-weld heat treated vessel plate seam welds in Reference 5, is used in this evaluation. The cosine distribution shown in Figure 2-16 is input into the appropriate flaw models.

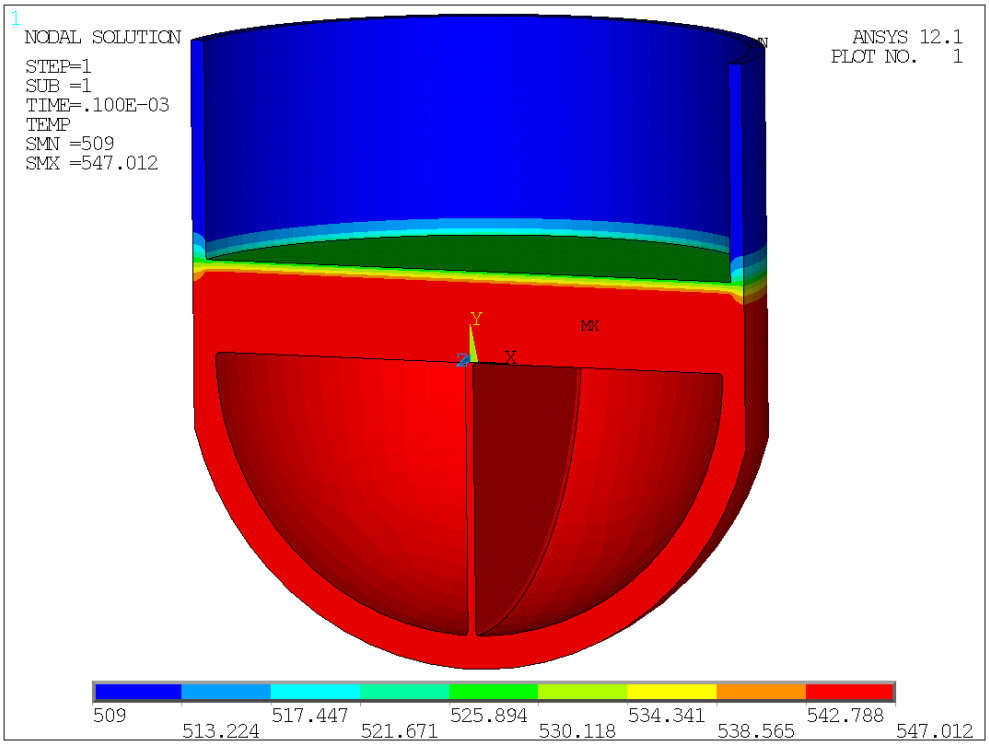

Figure 2-6
Sample Temperature Profile Results

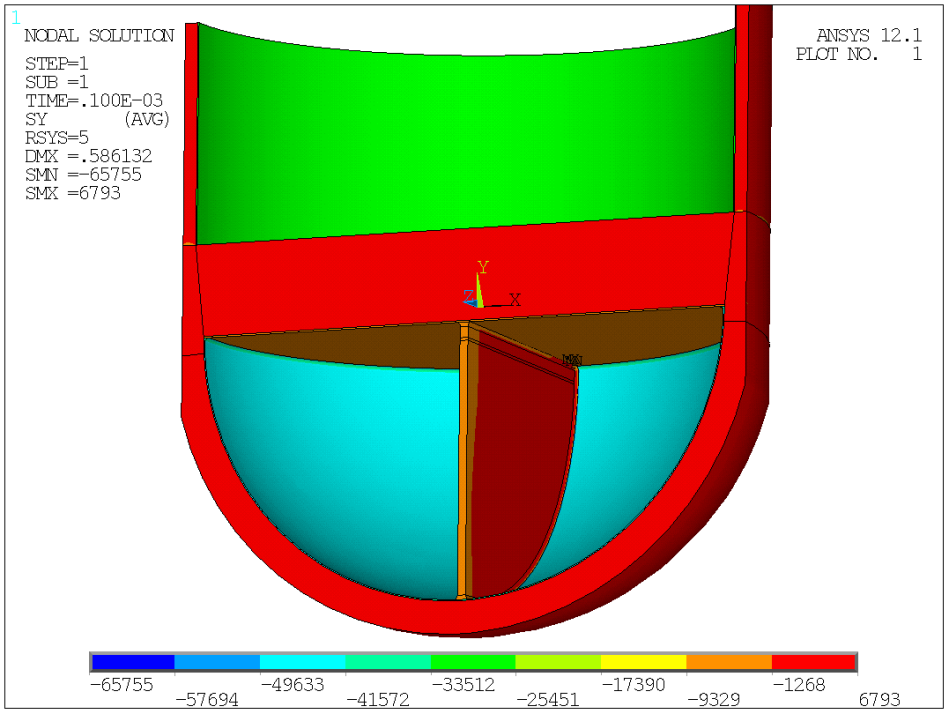

Figure 2-7
Sample Thermal Stress Results

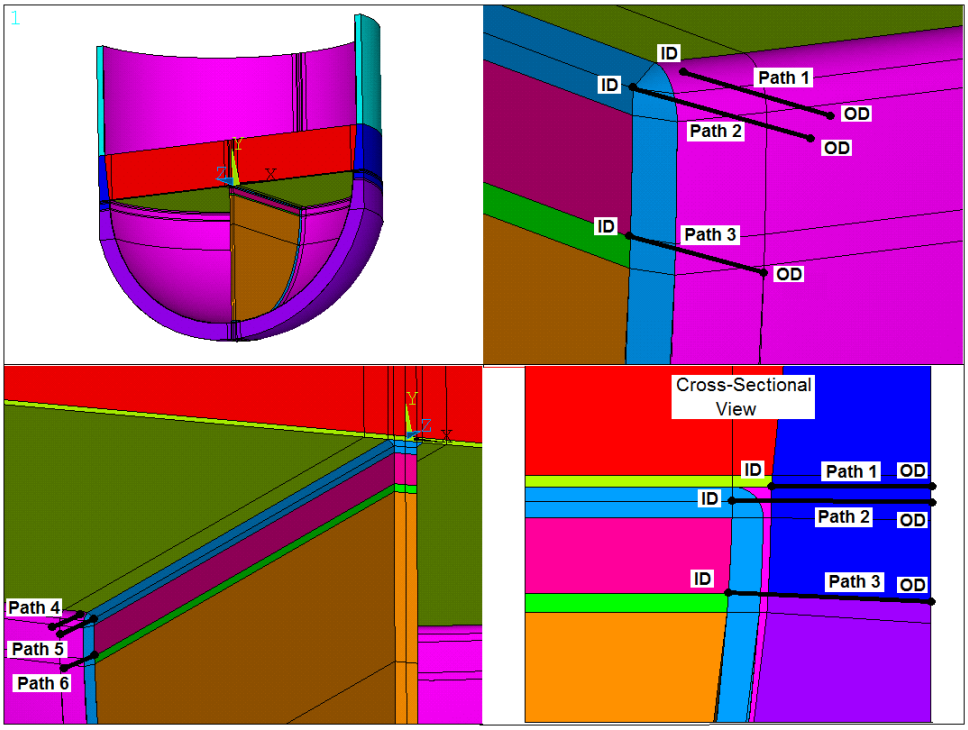

Figure 2-8
Through-Wall Paths for Stress Extraction

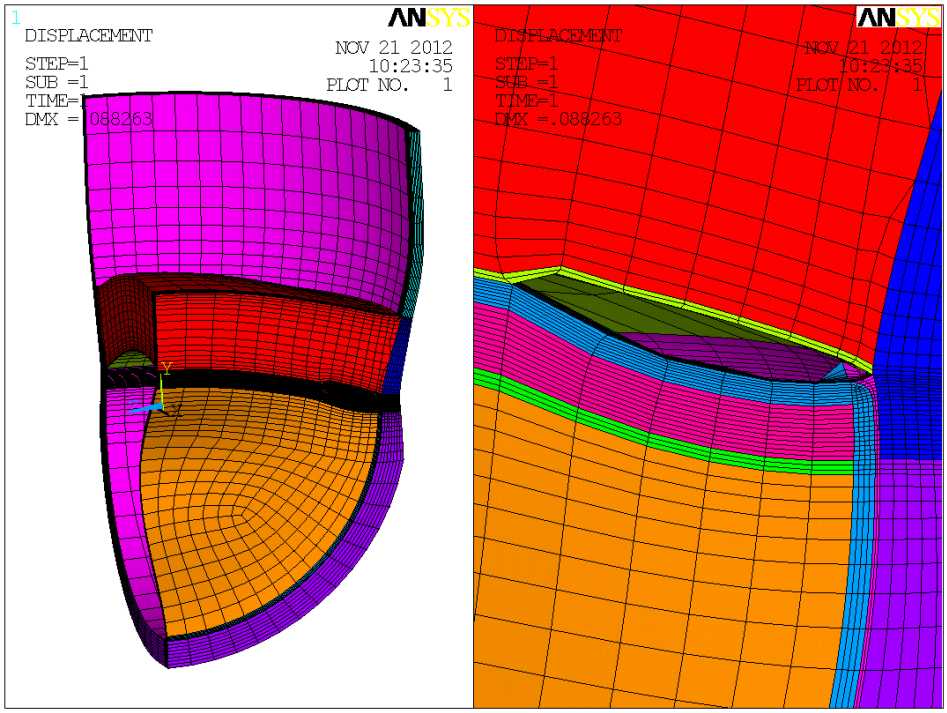

Figure 2-9
Exaggerated Displaced Shape Showing Crack Opening Due to Internal Pressure

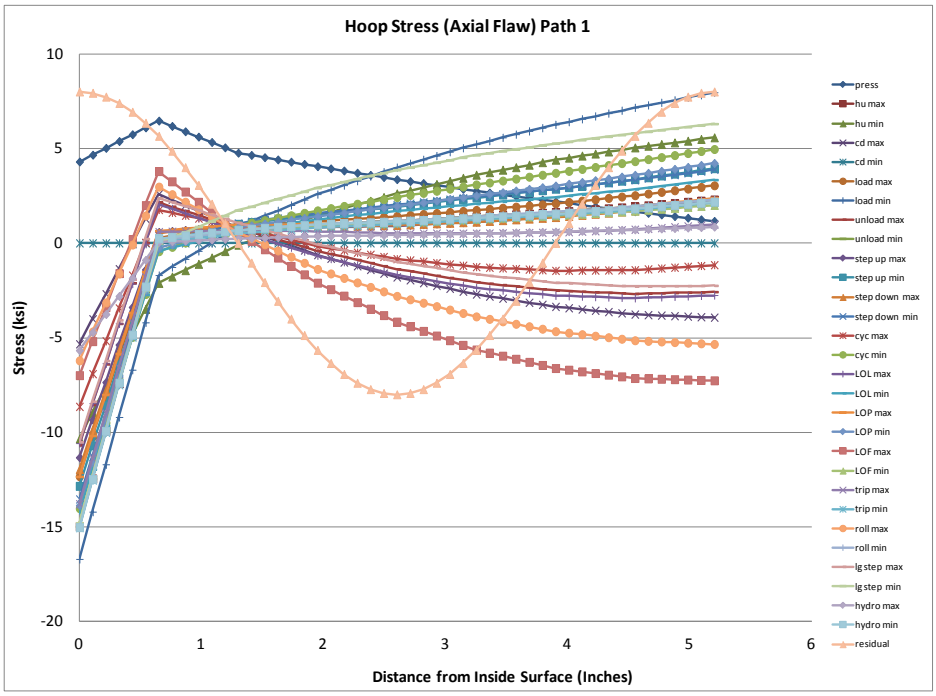

Figure 2-10
Hoop Stress Distributions at Path 1

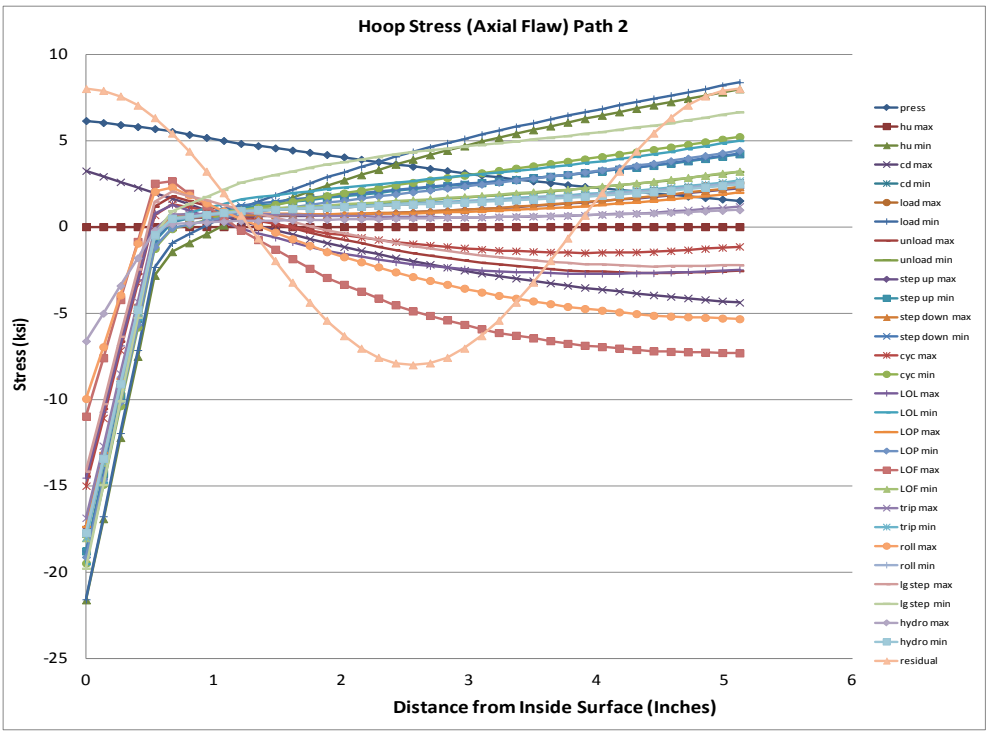

Figure 2-11
Hoop Stress Distributions at Path 2

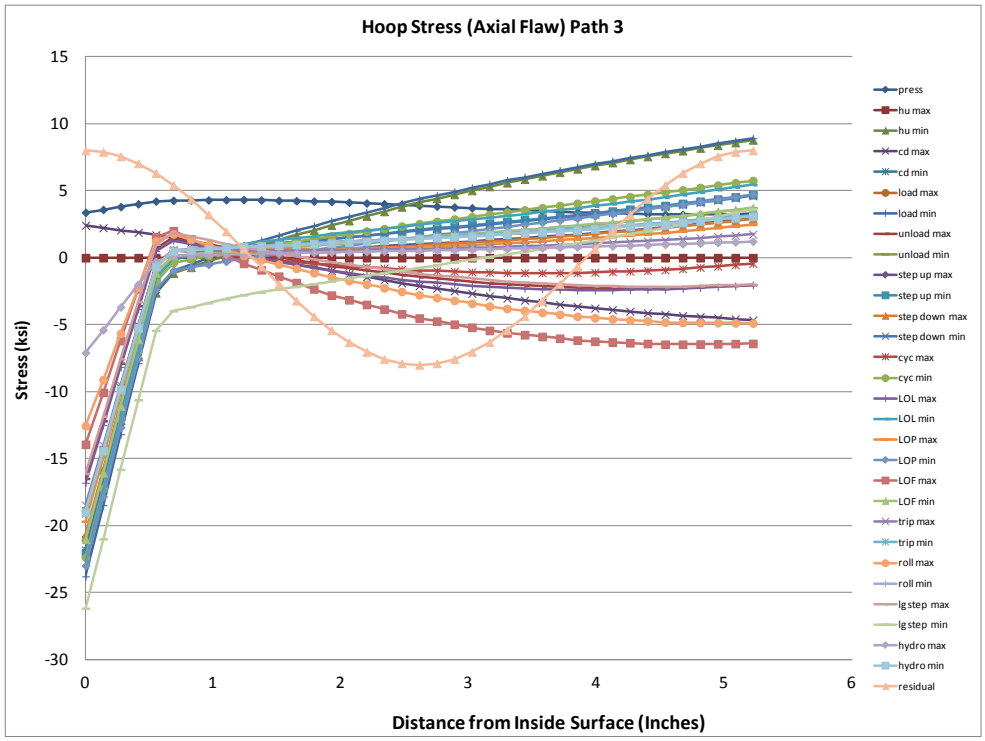

Figure 2-12
Hoop Stress Distributions at Path 3

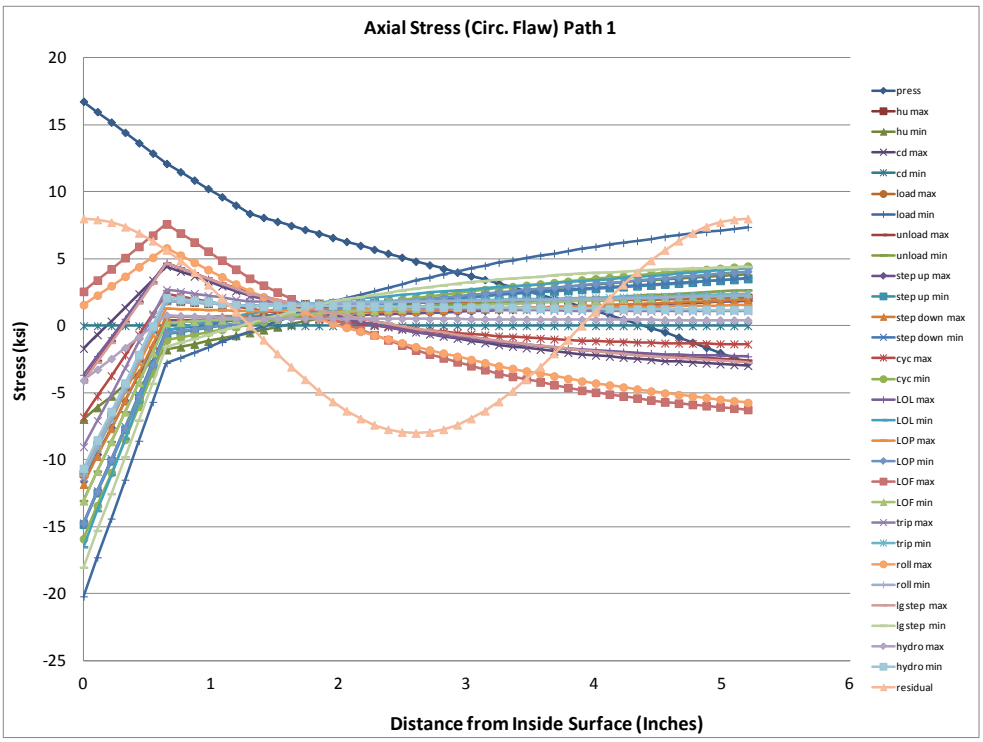

Figure 2-13
Axial Stress Distributions at Path 1

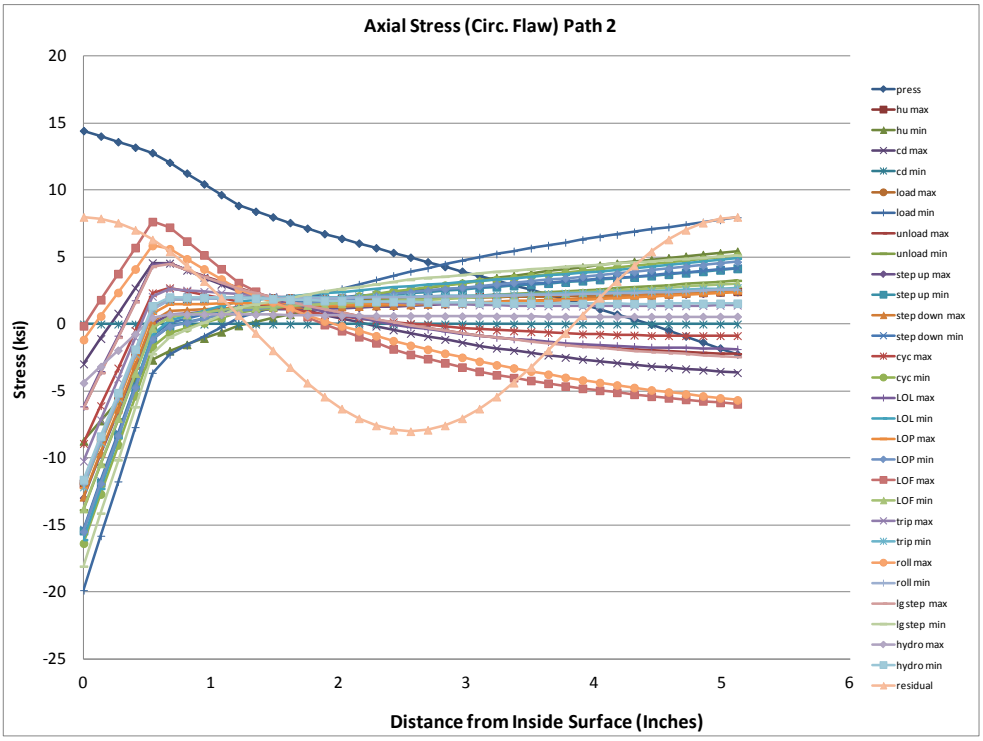

Figure 2-14
Axial Stress Distributions at Path 2

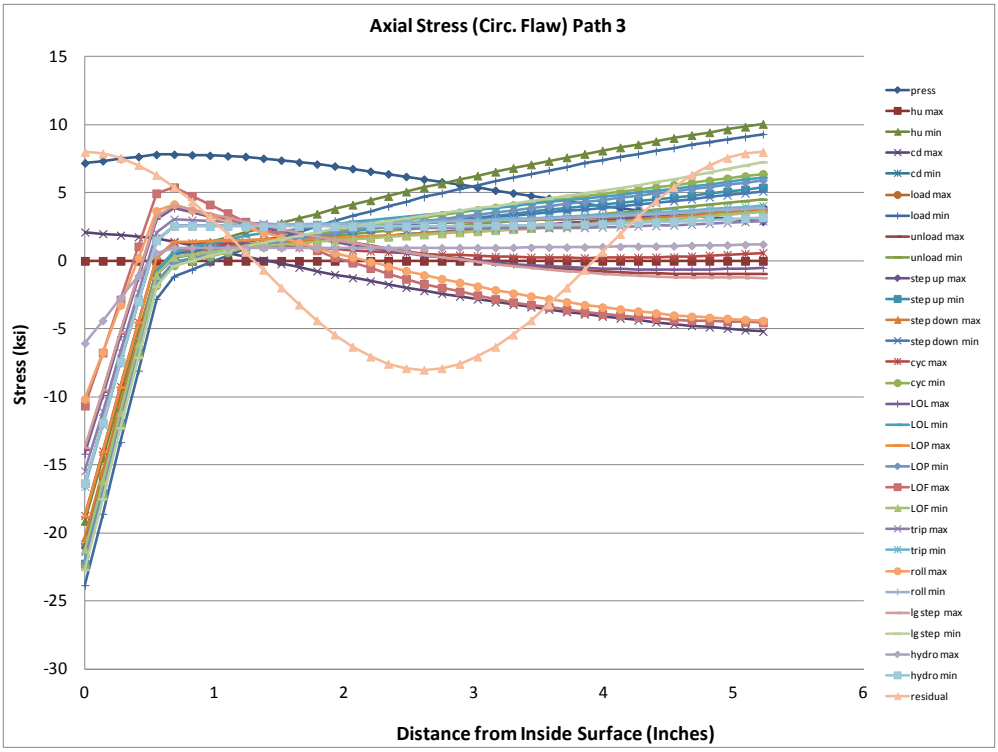

Figure 2-15
Axial Stress Distributions at Path 3

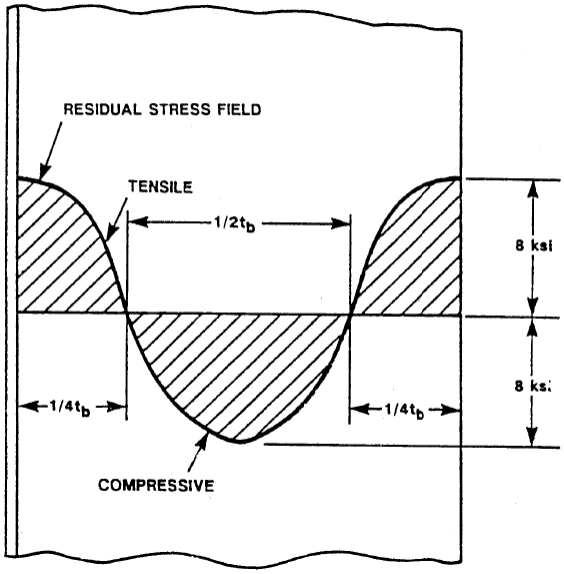

Figure 2-16
Weld Residual Stress Distribution

3
FRACTURE MECHANICS EVALUATION

Fracture mechanics analyses are performed to determine the flaw tolerance of the steam generator channel head using the finite element stress results described in Section 2.

Stress Intensity Factors

Two standard crack models are used in the evaluation to calculate stress intensity factors (K) due to all the applied loads for the postulated axial and circumferential flaws:

1. Semi-Elliptical Longitudinal Crack in Cylinder on the Inside Surface
2. Semi-Elliptical Circumferential Crack in Cylinder on the Inside Surface

The crack models and relevant variable parameters are depicted in Figure 3-1 and Figure 3-2.

The total K (at the deepest point of the flaw) is determined for each transient condition using the critical flaw size module within the fracture mechanics software **pc-CRACK™** [4] developed by Structural Integrity Associates. For each transient, the K values due to the thermal stress, corresponding pressure stress, and residual stress are applied, where the pressure is factored as shown in Table 3-1. The through-wall hoop stresses at the critical paths plotted in Figure 2-10, Figure 2-11 and Figure 2-12 are used for the axial crack models. Likewise, the critical through-wall axial stresses presented in Figure 2-13, Figure 2-14 and Figure 2-15 are used for the circumferential crack models.

As stated previously, since the proximity of the channel head seam welds to the triple point flaw location is unknown, the flaw evaluations are conservatively performed with the weld residual stress distribution specified in Figure 2-16 [5].

The postulated ID-connected elliptical flaws are assumed to have initial flaw depth, a, of 0.25 inches, equal to the clad thickness), and a flaw length, l, of 1.9 inches, equal to the divider plate thickness ($l = 2c$ in Figure 3-1 and Figure 3-2). This assumption, based on modeled component dimensions, corresponds to a longer initial flaw than if the aspect ratio of $a/l = 1/6$ recommended by ASME Code Section XI, Table L-3210-1 [2] had been used.

For all transients (except the heatup and cooldown transients), the thermal transient stresses are extracted at the time of maximum (or minimum) linearized membrane-plus-bending thermal stress (time of maximum thermal stresses). The maximum (or minimum) pressure is then conservatively applied in the loading blocks shown in Table 3-1. The stresses for the heatup and cooldown transients are reported at times of maximum total (thermal plus coincident pressure) linearized membrane-plus-bending stress. Therefore, the K due to internal pressure alone is factored by the values shown in Table 3-1.

For each load case (transient), the total stress intensity factor includes stresses due to weld residual stress, internal pressure, and thermal transient loadings (stresses shown in Figure 2-10 through Figure 2-15). The resulting maximum and minimum total stress intensity factors (K) used in the evaluations are plotted in Figure 3-3, Figure 3-4 and Figure 3-5 for the axially cracked cylinder models, and in Figure 3-6, Figure 3-7 and Figure 3-8 for the circumferentially cracked cylinder models. The results shown in these figures include the weld residual stresses.

Table 3-1
Load Cases

		Max. Load Combo.			Min. Load Combo.			Cycles per year
Event #		Thermal ID	Residual	Pressure Factor	Thermal ID	Residual	Pressure Factor	
1	Heatup(1)	HU_MX	RESID	See Note 1	HU_MN	RESID	See Note 1	5
2	Cooldown(1)	CD_MX	RESID	See Note 1	CD_MN	RESID	See Note 1	5
3	Load	LOAD_MX	RESID	1.0	LOAD_MN	RESID	1.0	458
4	Unload	UNLOAD_MX	RESID	1.0	UNLOAD_MN	RESID	1.0	458
5	Step up	STPU_MX	RESID	1.030	STPU_MN	RESID	0.971	50
6	Step down	STPD_MX	RESID	1.033	STPD_MN	RESID	0.967	50
7	Cycling	CYC_MX	RESID	1.013	CYC_MN	RESID	0.989	625
8	Loss load	LOL_MX	RESID	1.133	LOL_MN	RESID	0.711	2
9	Loss power	LOP_MX	RESID	1.110	LOP_MN	RESID	0.920	1
10	LOF	LOF_MX	RESID	1.0	LOF_MN	RESID	0.833	2
11	Trip	TRIP_MX	RESID	1.0	TRIP_MN	RESID	0.831	10
12	Roll test	ROLL_MX	RESID	0.853	ROLL_MN	RESID	1.0	1
13	Hydro	HYD_MX	RESID	1.01	HYD_MN	RESID	0.00	4
14	Large step down	LGST_MX	RESID	1.044	LGST_MN	RESID	0.878	5

[1] The stresses from the heatup and cooldown stress evaluations are taken at times of maximum and minimum total (thermal plus coincident pressure) linearized membrane-plus-bending stress. The coincident pressures at these times are used, as reported in the Pressure Factor column. For the heatup and cooldown transients, the pressure factors are:

Transient	Stress State	Path 1		Path 2		Path 3	
		Axial	Circ	Axial	Circ	Axial	Circ
Heatup	Max	1.0	1.0	0.178	1.0	0.178	0.178
	Min	0.507	0.342	1.0	0.424	1.0	1.0
Cooldown	Max	0.753	0.753	0.178	0.836	0.178	0.178
	Min	0.178	0.178	1.0	0.178	1.0	1.0

[2] For all transients except heatup and cooldown, the maximum or minimum pressure is added to the maximum or minimum thermal stress results, regardless of the time during which the thermal stresses are extracted. Doing so conservatively maximizes the total stress range and ΔK, and slightly increases the total crack growth.

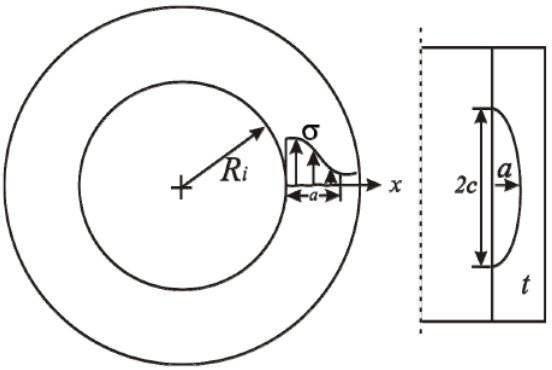

Stress/Load Input	
Stress Coefficients	✓
Coeffs. from Stress Table	✓
Stress Table	✓
Stress Intensity Factors (1D)	✓
Stress Intensity Factors (2D)	✓
Crack Dimensions: a c Component Dimensions: t R_i	
Range: $0.0 < a/t \leq 0.8$ $0.03125 \leq a/c \leq 2.0$ $0.0 < t/R_i \leq 1.0$	

Figure 3-1
Semi-Elliptical Longitudinal Crack in Cylinder on the Inside Surface

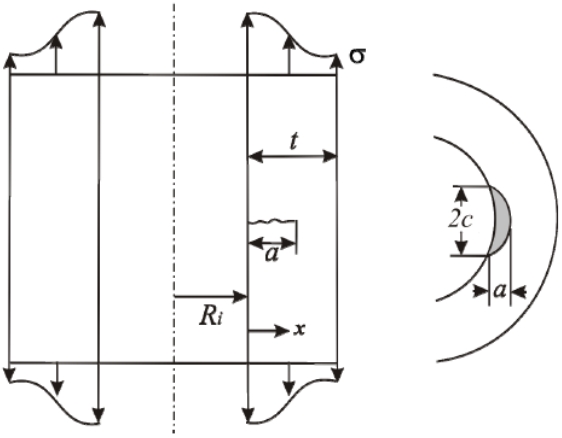

Stress/Load Input	
Stress Coefficients	✓
Coeffs. from Stress Table	✓
Stress Table	✓
Stress Intensity Factors (1D)	✓
Stress Intensity Factors (2D)	✓
Crack Dimensions: a c Component Dimensions: t R_i	
Range: $0.0 < a/t \leq 0.8$ $0.03125 \leq a/c \leq 2.0$ $0.0 < t/R_i < 1.0$ Source: [11]	

Figure 3-2
Semi-Elliptical Circumferential Crack in Cylinder on the Inside Surface

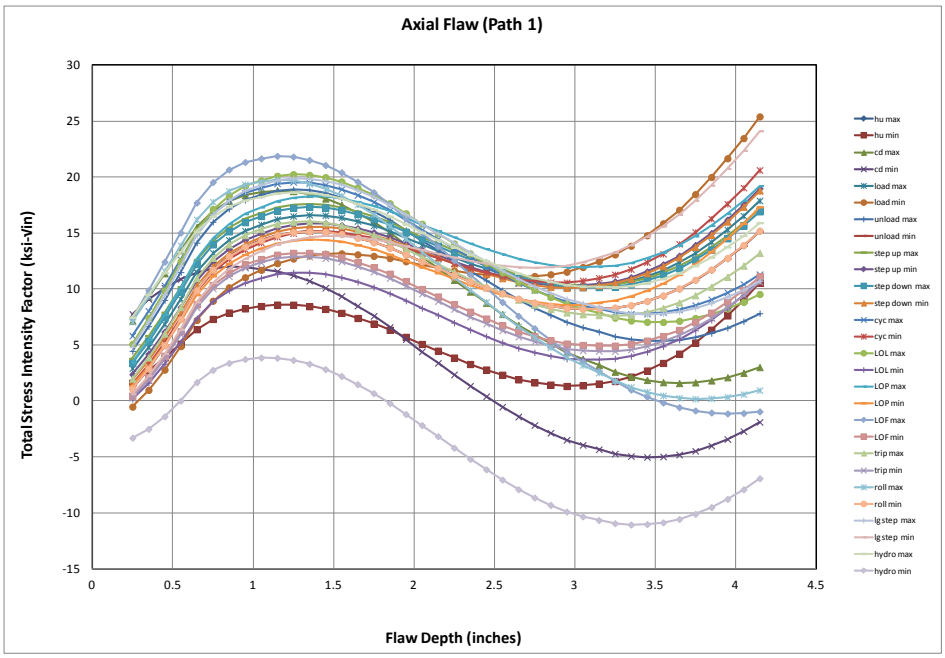

Figure 3-3
Total Stress Intensity Factor Results, Axial Flaw (Path 1)

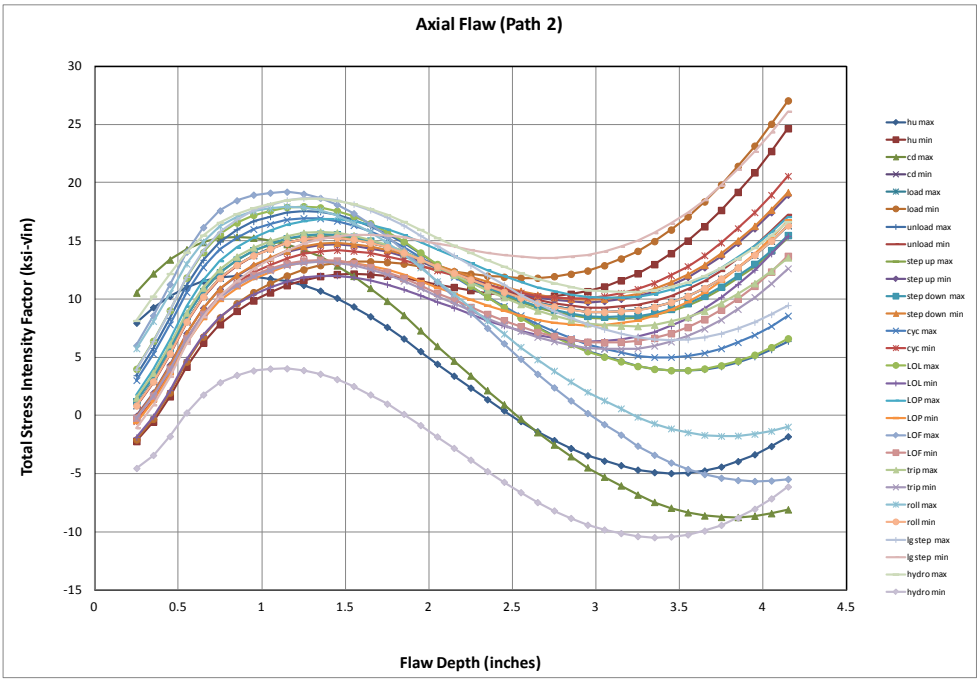

Figure 3-4
Total Stress Intensity Factor Results, Axial Flaw (Path 2)

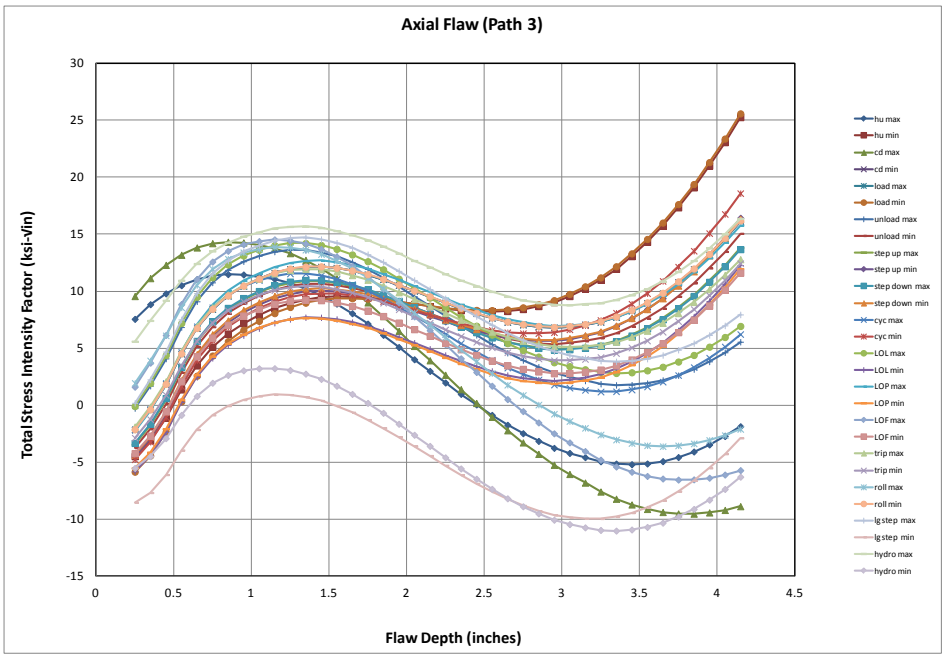

Figure 3-5
Total Stress Intensity Factor Results, Axial Flaw (Path 3)

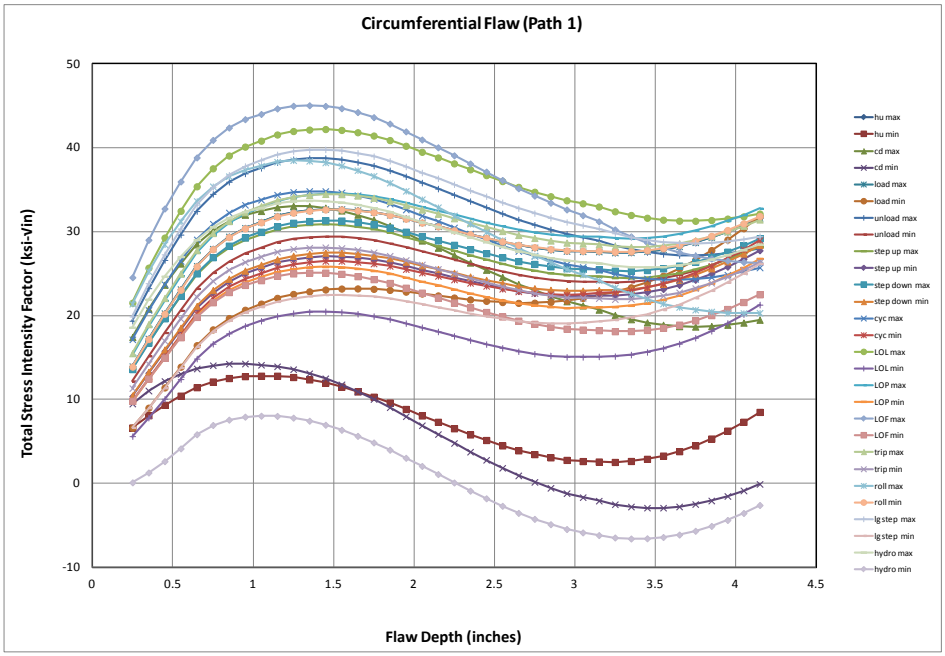

Figure 3-6
Total Stress Intensity Factor Results, Circumferential Flaw (Path 1)

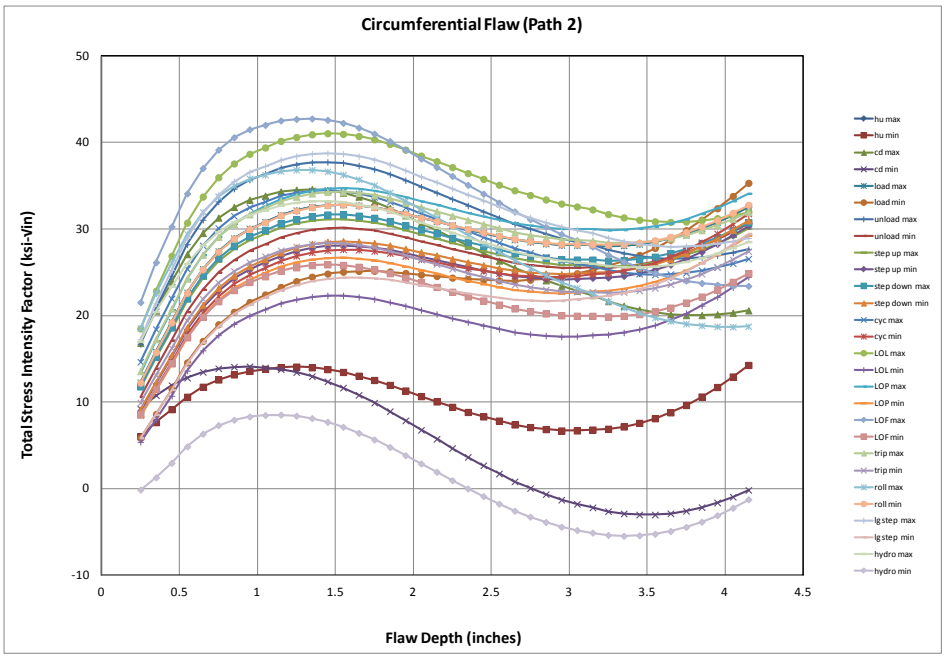

Figure 3-7
Total Stress Intensity Factor Results, Circumferential Flaw (Path 2)

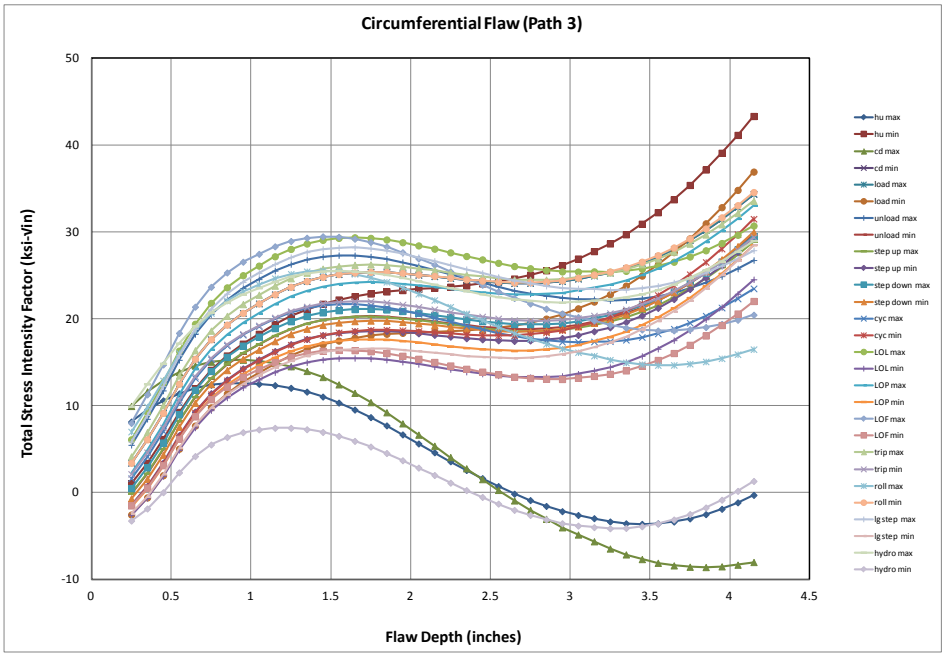

Figure 3-8
Total Stress Intensity Factor Results, Circumferential Flaw (Path 3)

Acceptance Criteria

The allowable flaw depth is determined using ASME Code Section XI, Appendix A methodology and IWB-3600 acceptance criteria [2].

Per ASME Code Section XI, IWB-3612 [2], any flaw exceeding the limits of IWB-3500 is acceptable if the applied stress intensity factor and the flaw size satisfy the following criteria:

a) For normal conditions:

$$K_I < K_{Ic}/\sqrt{10}$$

b) For emergency/faulted conditions and conditions where pressurization does not exceed 20% of the Design Pressure:

$$K_I < K_{Ic} / \sqrt{2}$$

Where:

K_I = the maximum applied total stress intensity factor (including stress due to weld residual, pressure, and thermal loadings) for normal and upset (N/U) conditions, including test conditions, or emergency and faulted (E/F) conditions for the end-of-evaluation period flaw size.

K_{Ic} = fracture toughness based on crack initiation for the corresponding crack-tip temperature.

Per ASME Code Section XI, Article A-4200 [2, Figure A-4200-1], a lower bound curve for K_{Ic} is prescribed for low alloy/ferritic steels (shown in Figure 3-9) as:

$$K_{Ic} = 33.2 + 20.734 \exp[0.02(T - RT_{NDT})]$$

where, T is the evaluated metal temperature, and RT_{NDT} is the reference nil-ductility test temperature.

The maximum K_{Ic} is limited to an upper-shelf value of 200 ksi-√in. Since the RT_{NDT} value comes from test data and typically has a wide range of values for different materials, a range of values is evaluated, as shown in Figure 3-10. Values of 10°F and 50°F are chosen as conservative bounding values, along with representative values for the ferritic SA-216 WCC channel head material. For the SA-216 material, Reference 7 reports K_{Ic} = 155 ksi-√in at room temperature. The equivalent RT_{NDT} using the prescribed ASME curve fit (above) is approximately -18°F. Therefore, applying the lower bound ASME curve results in overly conservative estimates of the fracture toughness and allowable stress intensity factors.

Since most of the thermal transients (other than heatup and cooldown) are at elevated temperatures far above the upper shelf temperature corresponding to (T- RT_{NDT}) of 105°F at 200 ksi-√in, the allowable is K_{allow} = 63.2 ksi-$in^{1/2}$, for temperatures above (T – RT_{NDT}). For these transient conditions, the maximum allowable flaw size corresponds to flaw depths at which the allowable K of 63.2 ksi-$in^{1/2}$ is reached. As addressed below, for the elevated temperature conditions (i.e. above the upper shelf temperature of 105°F) evaluated, the IWB-3600 acceptance criteria are satisfied using the bounding curve given in ASME Code Section XI, Article A-4200 [2].

The initial and final maximum total applied K values are summarized in Table 3-2. As seen in Table 3-2, the bounding K values for the axial flaw are at Path 2 with a maximum K of 10.55 ksi-√in at the end of the 40-year evaluation period. The most limiting K values for the circumferential flaw are at Path 1 with a maximum K of 31.05 ksi-√in after 40 years of crack growth.

The results show that the maximum K is less than the allowable value of 63.2 ksi-√in for all transients (note that low temperature conditions during heatup and cooldown that can potentially lead to an allowable K of less than 63.2 ksi-√in are discussed below), for both axial and circumferential flaw types, up to 75% of the vessel wall thickness as shown in Figure 3-3 through Figure 3-8. Therefore, the allowable flaw depth is set to 75% of wall (a/t = 0.75).

Low Temperature/Low Pressure Conditions

The heatup and cooldown transients include low temperature conditions when the ductility of the channel head material falls below the upper shelf temperature, i.e. approximate T-RT_{NDT} = 105°F (see Figure 3-9). Since the allowable stress intensity factor becomes dependent on both temperature and pressure (per ASME Code Section XI, IWB-3612 [2], the allowable K increases from K_{Ic} /√10 to K_{Ic} /√2 at pressures below 20% of Design Pressure), conditions at these low temperature ranges must be evaluated. In order to assure the allowable criteria are met, stress results are extracted from both the heatup and cooldown transients near this critical transition point.

The axial and hoop stress results for the heatup transient are extracted for the following conditions, where 20% of the Design Pressure is taken to be 500 psi:

Time	Pressure	Metal Temperature	Allowable Criteria	
858 sec.	493 psi	76°F	K_{Ic} / √2	(P < 500 psi)
1,717 sec.	585 psi	87°F	K_{Ic} / √10	(N/U conditions; P > 500 psi)

Likewise for the cooldown transient, the following conditions are evaluated:

Time	Pressure	Metal Temperature	Allowable Criteria	
15,455 sec.	585 psi	115°F	K_{Ic} / √10	(N/U conditions; P > 500 psi)
17,172 sec.	400 psi	68°F	K_{Ic} / √2	(P < 500 psi)

As mentioned above, for the SA-216 material, Reference 7 reports K_{Ic} = 155 ksi-√in at room temperature. The equivalent RT_{NDT} using the prescribed ASME curve fit above is approximately -18°F. In addressing the low temperature/low pressure conditions occurring during the heatup and cooldown transients, the fracture toughness data given by Reference 7 is used in lieu of those prescribed in ASME, A-4200 (Figure 3-9), which produce extremely low allowable values at these low temperatures.

As seen in Figure 3-11, Figure 3-12 and Figure 3-13, the heatup conditions meet the allowable values, regardless of which fracture toughness curve is used for the allowable. Likewise, the allowable values are also met for all the cooldown conditions, as shown in Figure 3-14, Figure 3-15 and Figure 3-16.

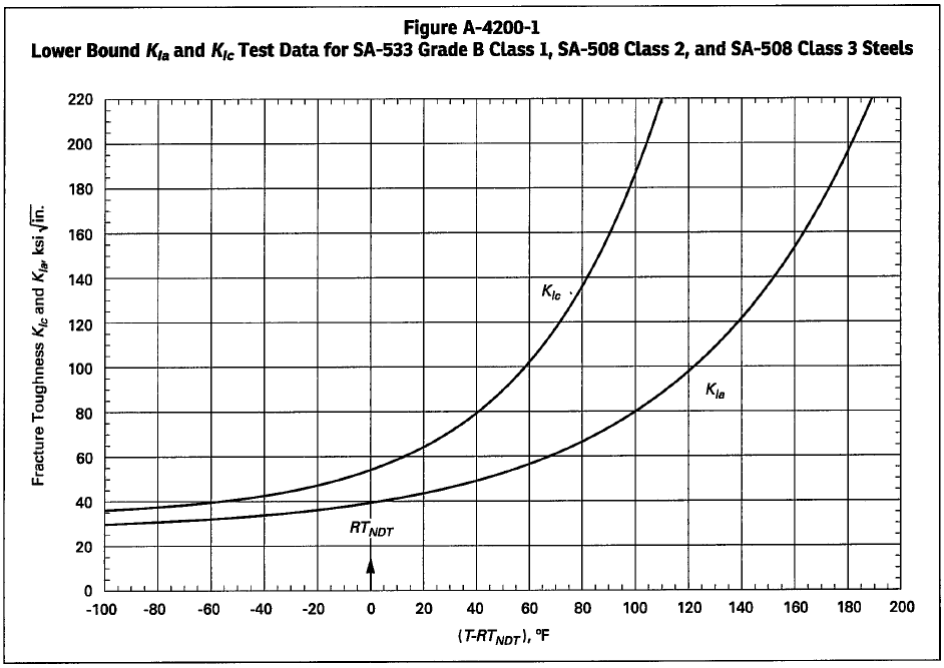

Figure 3-9
Lower Bound Fracture Toughness Curve (ASME Code Section XI)

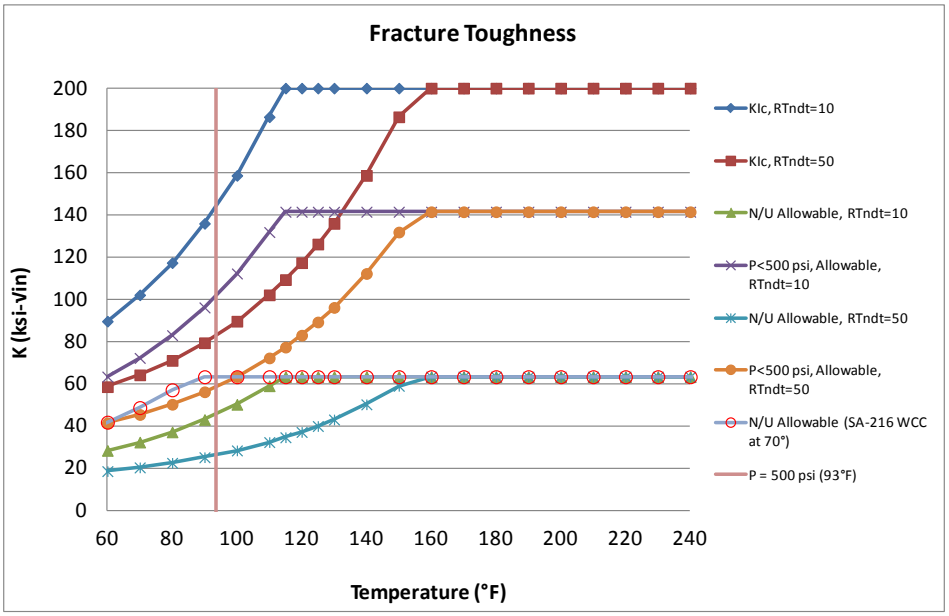

Note: The curve for SA-216 WCC is generated using the ASME Code equation for low alloy steel, where the RT_{NDT} value of -18°F corresponds to K_{Ic} = 155 ksi-√in at room temperature. The corresponding normal/upset allowable K is therefore taken to be $K_{Ic}/\sqrt{10}$ = 49 ksi-√in at 70°F.

Figure 3-10
Temperature-Dependent Fracture Toughness Values

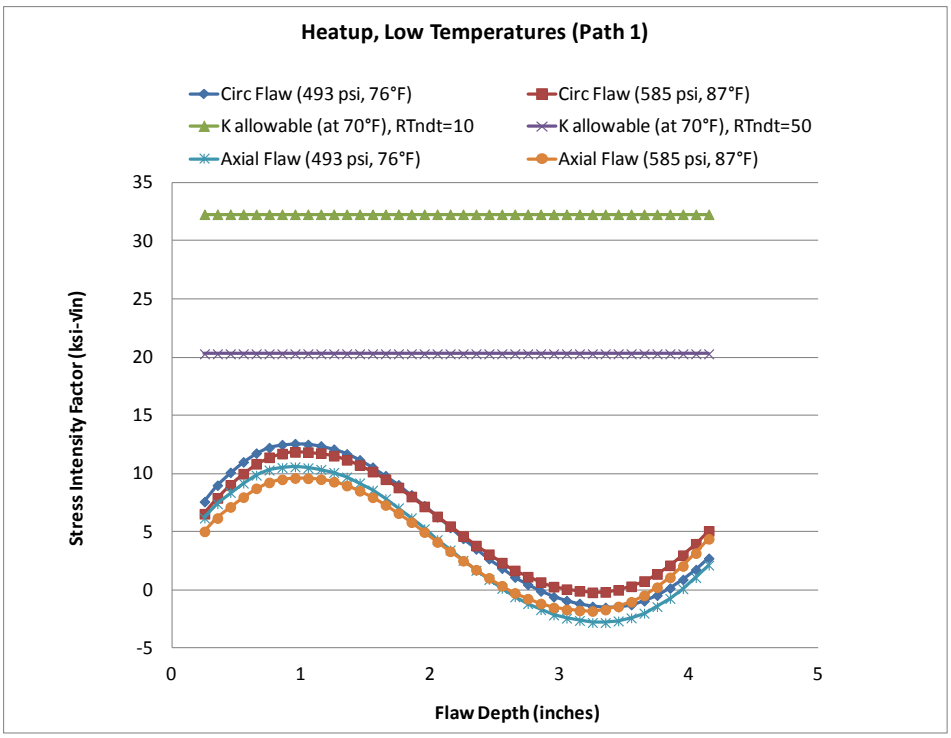

Figure 3-11
Heatup Deep Point K at Low Temperature (Path 1)

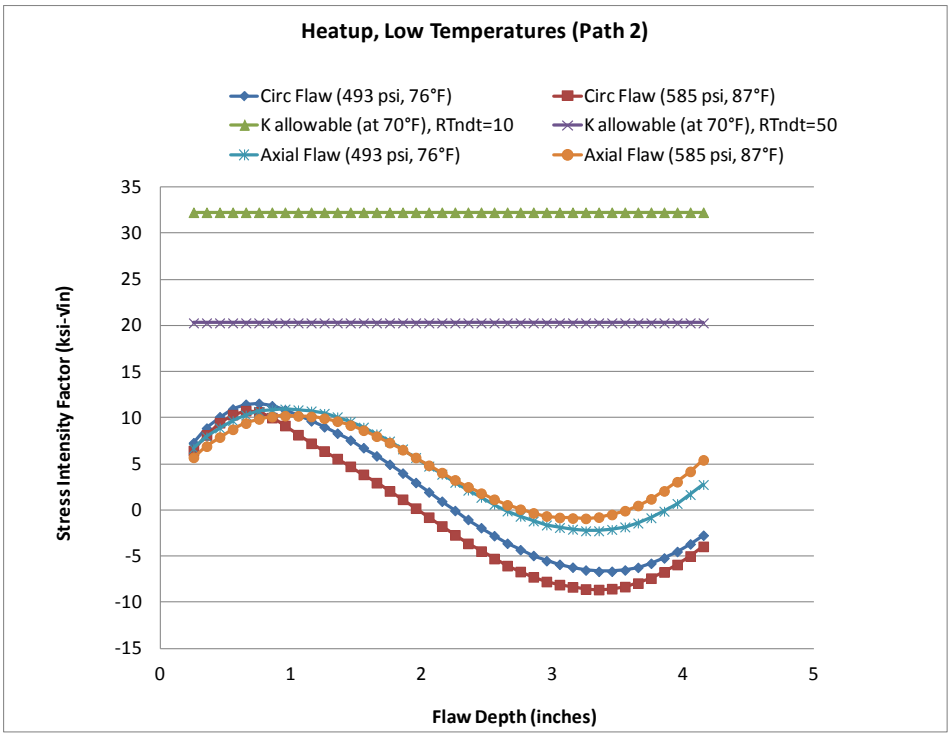

Figure 3-12
Heatup Deep Point K at Low Temperature (Path 2)

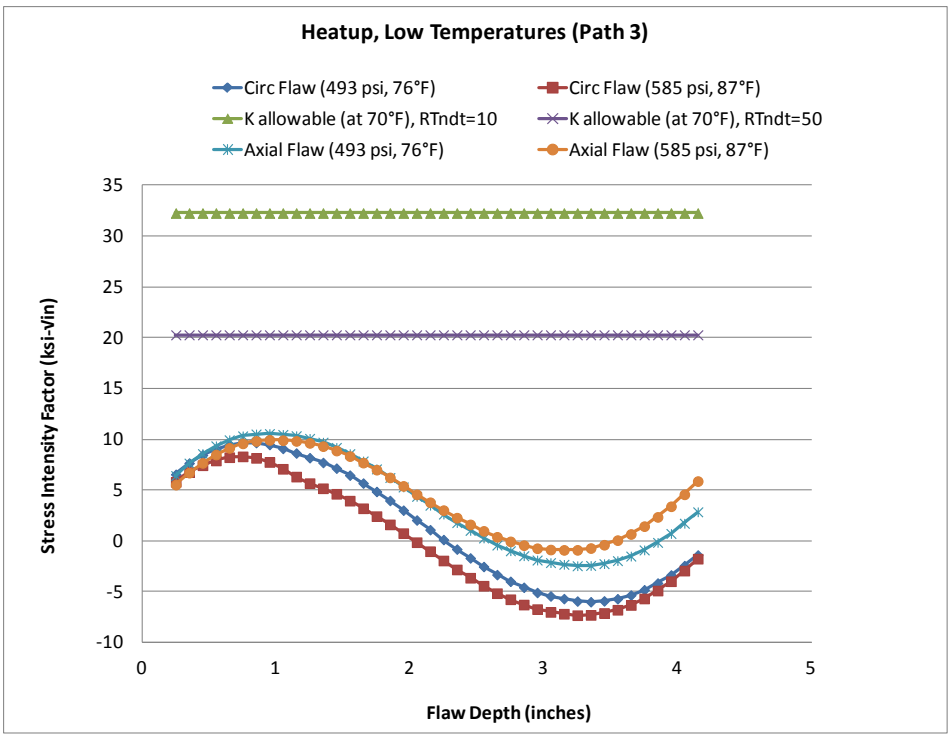

Figure 3-13
Heatup Deep Point K at Low Temperature (Path 3)

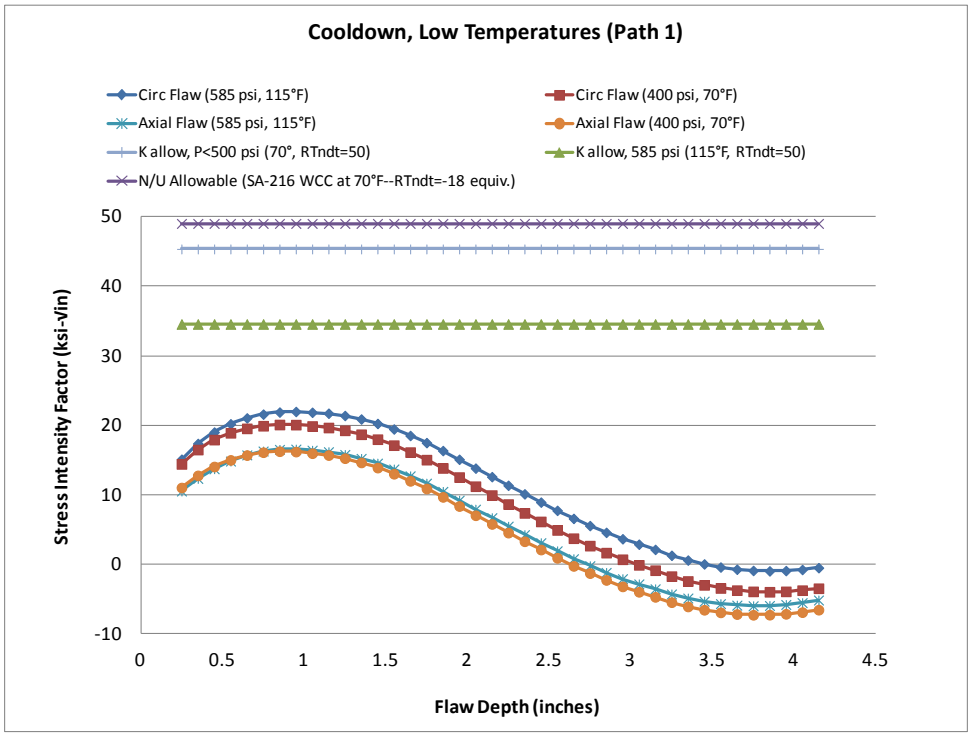

Figure 3-14
Cooldown Deep Point K at Low Temperature (Path 1)

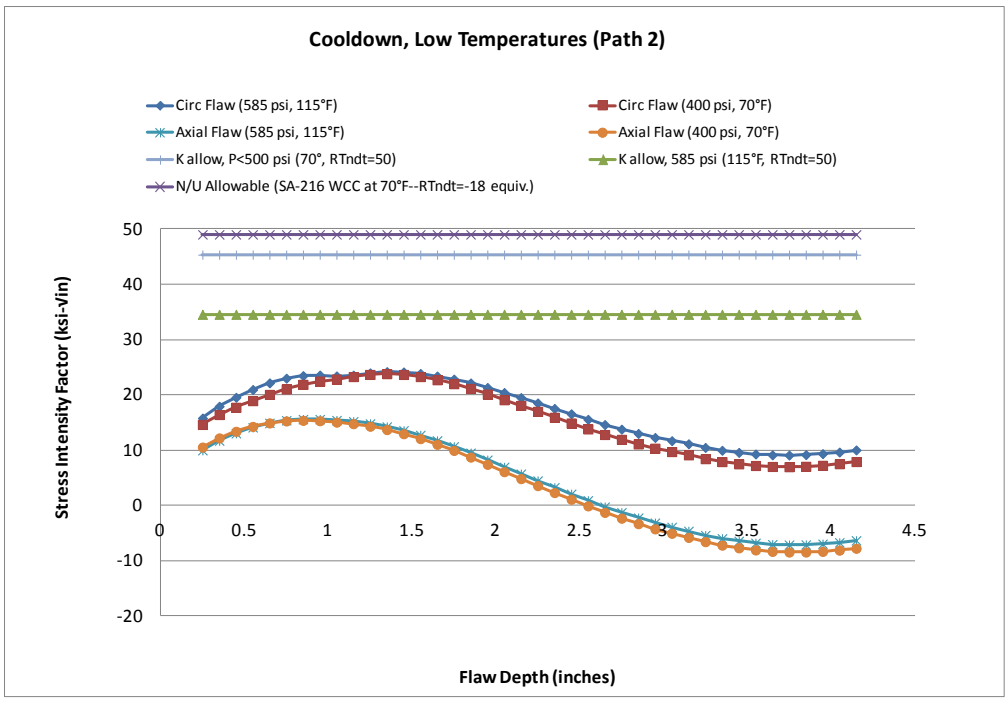

Figure 3-15
Cooldown Deep Point K at Low Temperature (Path 2)

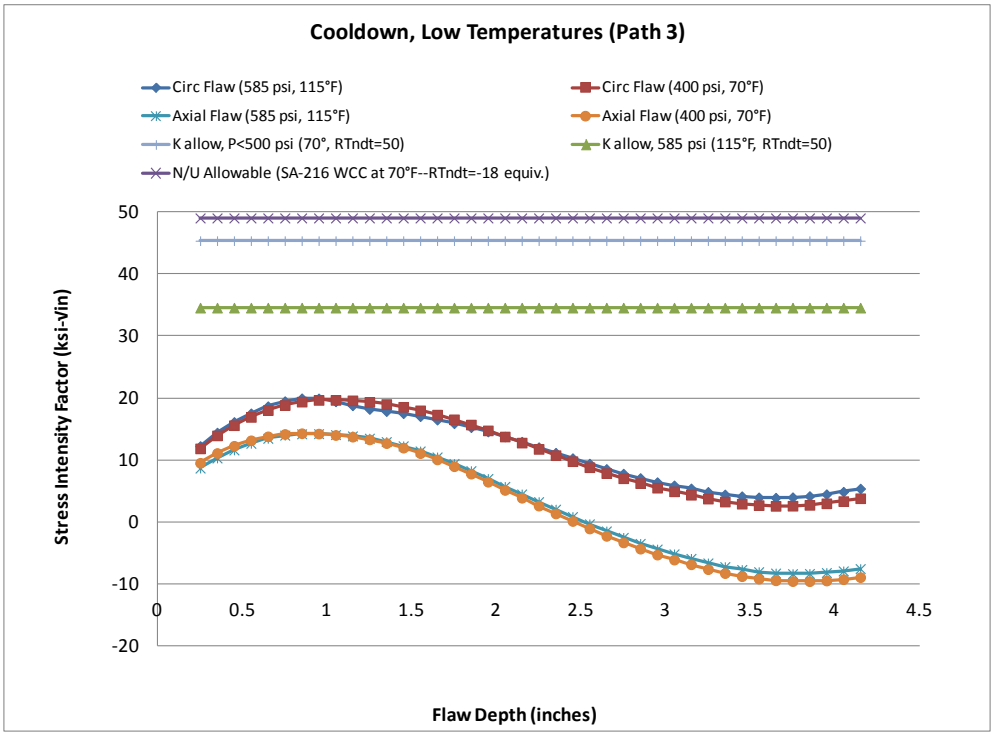

Figure 3-16
Cooldown Deep Point K at Low Temperature (Path 3)

Fatigue Crack Growth Analysis

A fatigue crack growth evaluation is performed for hypothesized axial and circumferential ID-connected flaws in the steam generator channel head, initiating at the bounding triple point location. These postulated flaws can potentially grow due to cyclic fatigue loading. The methodology of Section XI, Appendix A of the ASME Code [2] is used to perform the fatigue crack growth analysis. The fatigue crack growth analysis is performed using the **pc-CRACK™** [4] fracture mechanics software. The analysis is performed using the pressure and transient stress results that were derived in Section 2. The crack growth evaluation is performed using the stress intensity factors (Ks) determined above.

Fatigue Crack Growth Rate

The fatigue crack growth rate (da/dN) for the carbon steel steam generator head material is a function of the range of applied stress intensity factor (ΔK_I) that can be expressed in the form of a Paris law. Since the flaws are assumed to initiate at the inside surface of the vessel/divider plate weld, the postulated flaws are exposed to the steam generator water environment. Hence, the ASME Code fatigue crack growth curves for ferritic and low alloy steels in water environments are used.

The fatigue crack growth law for ferritic material exposed to water environment given in Subarticle A-4300 of Section XI of the ASME Code [2] is expressed as follows:

$$da/dN = C_o(\Delta K_I)^n, \text{ units of inch/cycles}$$

where:

for low ΔK_I values:

$n = 5.95$
$C_o = 1.02 \times 10^{-12} S$
$S = 1.0$ for $0 \le R \le 0.25$
$= 26.9R - 5.725$ for $0.25 \le R \le 0.65$
$= 11.76$ for $0.65 \le R \le 1.0$
R = R-ratio = K_{min}/K_{max} (if $K_{min} \le 0$, then $R = 0$)
$\Delta K_I = K_{max} - K_{min}$ = range of applied K, ksi$\sqrt{in}$

for high ΔK_I values:

$n = 1.95$
$C_o = 1.01 \times 10^{-7} S$
$S = 1.0$ for $0 \le R \le 0.25$
$= 3.75R + 0.06$ for $0.25 \le R \le 0.65$
$= 2.5$ for $0.65 \le R \le 1.0$
R = R-ratio = K_{min}/K_{max} (if $K_{min} \le 0$, then $R = 0$)
$\Delta K_I = K_{max} - K_{min}$ = range of applied K, ksi$\sqrt{in}$

The value of ΔK_I is checked against the following, depending on the value of R:

$$\Delta K_I = 17.74 \qquad (0 \le R \le 0.25)$$
$$\Delta K_I = 17.74*[(3.75R + 0.06)/(26.9R - 5.725)]^{0.25} \qquad (0.25 < R < 0.65)$$
$$\Delta K_I = 12.04 \qquad (0.65 \le R \le 1.0)$$

As indicated in Subarticle A-4300 of Section XI of the ASME Code [2], if ΔK_I is less than this value, the parameters for low ΔK_I values are applied; otherwise, the parameters for high ΔK_I values are applied.

A threshold ΔK_I value of zero is conservatively assumed for the fatigue crack growth analyses.

The Ks determined for the various applied loads are linearly superimposed to determine the total maximum and minimum K values, from which the ΔK ranges for each transient are determined. The ΔK ranges are input into the above crack growth laws to compute the crack growth. Crack growth is based on a yearly block. The yearly cycles per transient are derived from the 40-year design basis cycles listed in Table 2-2 and Table 2-3, for the typical steam generator. In the event that the resultant number of cycles is a fraction, the decimal is rounded up to the nearest integer. The sequence of events and number of cycles for a one-year block are shown in Table 3-1. This number of yearly cycles is entered into the crack growth module of **pc-CRACK™** [4].

Initial Flaw Size Assumption

The initial flaw size is postulated based on component dimensions. Since the flaw is postulated to emanate from a crack in the divider plate, an initial flaw depth equal to the cladding thickness, a = 0.25" is assumed for the evaluations of crack propagation into the channel head wall. The flaw length is set equal to the divider plate thickness, 1.9", since the flaw is postulated to emanate from a through-wall crack in the divider plate. Therefore the flaw aspect ratio is 1.9/0.25 = 7.6. This ratio is conservatively larger than the 6:1 ratio recommended in ASME Code Section XI, Appendix L.

Fatigue Crack Growth Analysis Results

The results of the fatigue crack growth evaluations are tabulated in Table 3-2 for the different postulated crack geometries. The maximum fatigue crack growth and stress intensity factors are discussed in the following paragraphs.

The postulated initial circumferential flaw is predicted to grow from 0.25 inches to 0.404 inches (at Path 1) in 40 years. This is equivalent to 8% of the vessel wall thickness (i.e., a/t = 0.08)

The axial flaw types are less limiting, with the final flaw predicted to be 0.2514 inches (Path 3) after 40 years.

Since a flaw aspect ratio of a/l = 7.6 was assumed for the evaluations, the final limiting circumferential flaw depth of a = 0.404 inches corresponds to a circumferential flaw length of approximately l = 3.07 inches. Likewise, the maximum final axial flaw depth of a = 0.2514 inches corresponds to an axial flaw length of approximately l = 1.91 inches in the vertical direction of the channel head.

The results for 40 years of crack growth are plotted in Figure 3-17 for the circumferential flaws. Likewise, the axial flaw results are shown in Figure 3-18.

The initial and final maximum total applied K values for elevated temperature conditions are summarized in Table 3-2. The results show that the maximum stress intensity factor, K, is less than the allowable values for all transients, for both axial and circumferential flaws. Additionally, all K values for flaw depths up to 75% of the vessel wall thickness are below the allowable values as shown in Figure 3-3 through Figure 3-8. Therefore, the allowable flaw depth is 75% of the channel head base metal thickness (a/t = 0.75).

Table 3-2
Fracture Mechanics Analysis Result Summary

Results for 40 Year Crack Growth Period								
Stress Case	Flaw Type	Initial Flaw Depth (inch)	Final Flaw Depth (a) (inch)	Final Flaw Depth/Vessel Thickness (a/t)	Initial K max. (ksi-√in)	Final K max. (ksi-√in)	Allowable K (ksi-√in)	Pass?
Path 1 (with residual)	Circ	0.25	0.4040	0.080	24.632	31.048	63.2	Yes
	Axial	0.25	0.2508	0.048	7.465	7.482	63.2	Yes
Path 2 (with residual)	Circ	0.25	0.2985	0.057	21.555	23.806	63.2	Yes
	Axial	0.25	0.2510	0.048	10.527	10.545	63.2	Yes
Path 3 (with residual)	Circ	0.25	0.2524	0.049	9.954	9.998	63.2	Yes
	Axial	0.25	0.2514	0.048	9.555	9.579	63.2	Yes

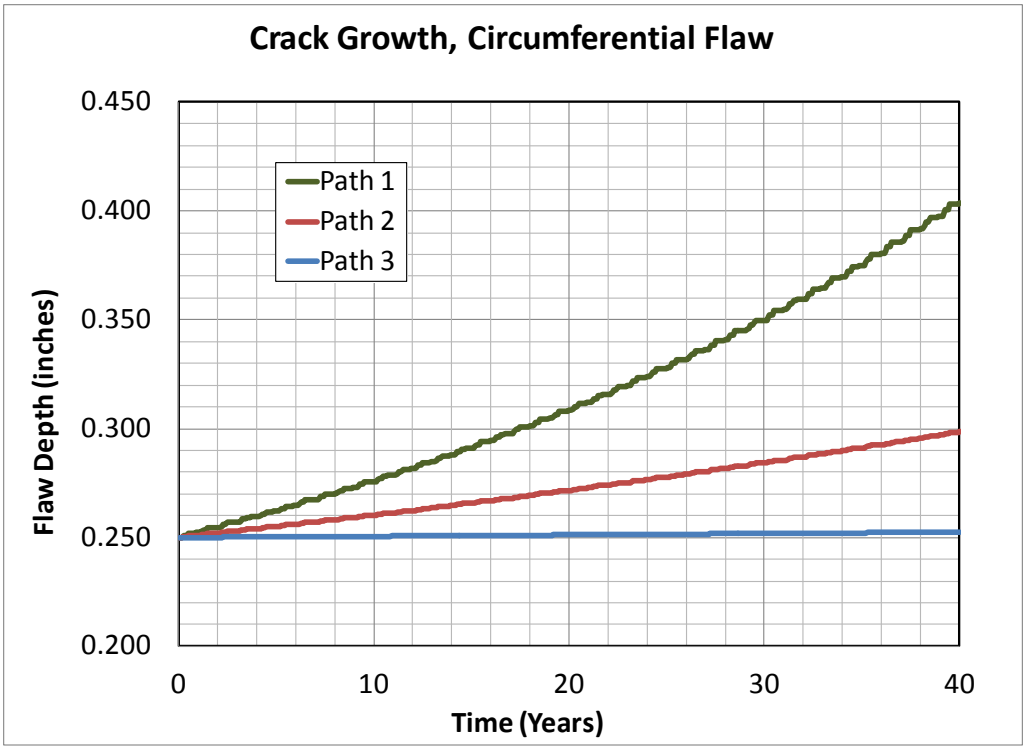

Figure 3-17
Bounding Crack Growth, Circumferential Flaw

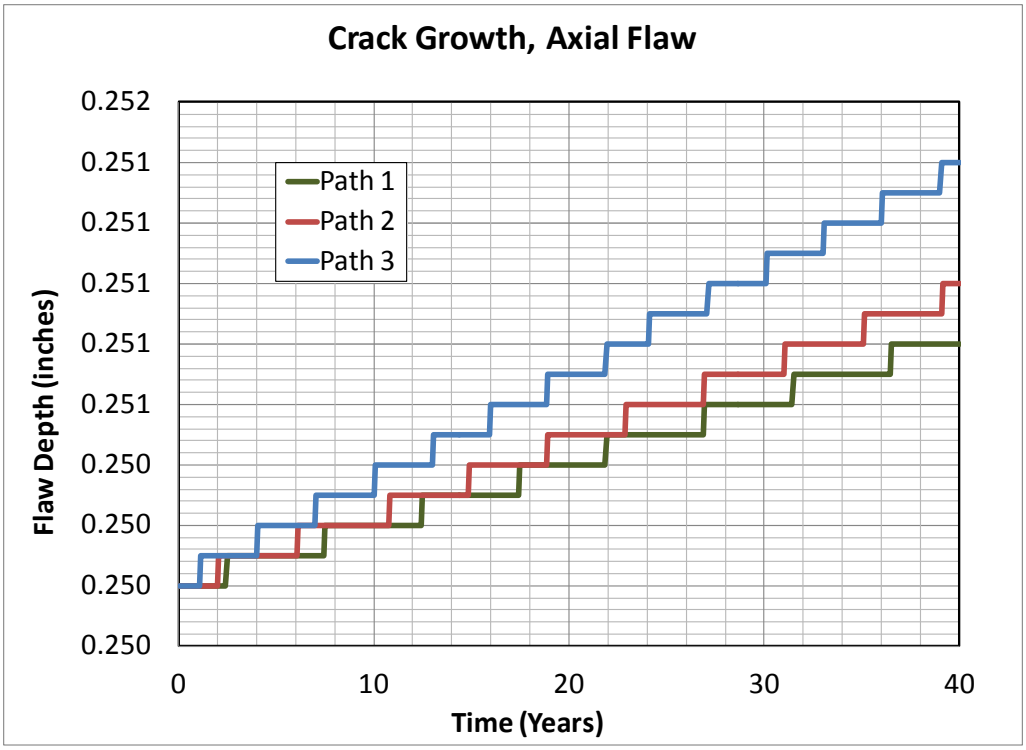

Figure 3-18
Bounding Crack Growth, Axial Flaw

4
CONCLUSIONS

A representative finite element model of the steam generator channel head was evaluated, and typical design transients evaluated. Stress paths were defined through the steam generator channel head wall, around the region of the attached divider plate weld. Mapped through-wall hoop and axial stresses along these paths were extracted, and the results used to perform fracture mechanics and fatigue crack growth evaluations.

The results show that the maximum stress intensity factor, K, is less than the allowable values for all design basis plant conditions, for both axial and circumferential flaw types, up to 75% of the vessel wall thickness. Therefore, the allowable flaw depth is taken as 75% of the channel head base metal thickness (a/t = 0.75), i.e., 3.9 inches.

A fatigue crack growth evaluation was performed for postulated axial and circumferential flaws in the steam generator channel head, initiating at the bounding triple point location of the channel head assembly. A postulated 0.25 inch deep initial circumferential flaw is predicted to grow to a maximum depth of 0.404 inches and maximum length of 3.07 inches in 40 years of operation. Similarly, a postulated 0.25 inch deep initial axial flaw is predicted to grow to a maximum depth of 0.25140 inches and maximum length of 1.91 inches in 40 years of operation. The final crack depths remain well below the allowable flaw depth of 3.9 inches.

The flaw tolerance evaluation summarized herein has demonstrated that the structural integrity of the steam generator channel head is not compromised by a crack in the divider plate. The evaluation includes several design input assumptions based on industry data or engineering judgment which are generally conservative. Some assumptions such as the postulated ¼" initial flaw in the channel head wall and the approximately 15-inch long through-wall crack in the divider plate are conservative and could be reassessed if more information from plant experience becomes available. The assumption of the location of the through-wall crack in the divider plate in this evaluation was based on critical stress results at the tubesheet-to-stub runner full penetration weld (triple-point location) in an uncracked steam generator channel head assembly.

5
REFERENCES

1. *Divider Plate Cracking in Steam Generators: Results of Phase 1: Analysis of Primary Water Stress Corrosion Cracking and Mechanical Fatigue in the Alloy 600 Stub Runner to Divider Plate Weld Material*. EPRI, Palo Alto, CA: 2007. 1014982.
2. ASME Boiler and Pressure Vessel Code, Section II, Part D and Section XI, 2010 Edition w/2011 Addenda.
3. ANSYS Mechanical APDL and PrepPost, Release 12.1 x64, ANSYS, Inc., November 2009.
4. **pc-CRACK**, Version 4.0.1.0, Structural Integrity Associates, December 14, 2011.
5. Electric Power Research Institute (EPRI, Palo Alto, CA) Report # TR-100251, Project 2975-13, January 1993, “White Paper on Reactor Vessel Integrity Requirements for Level A and Level B Conditions.”
6. American Petroleum Institute (API), API-579-1/ASME FFS-1 Fitness-For-Service 2007, Annex C, “Compendium of Stress Intensity Factor Solutions.”
7. Steel Founders’ Society of America, Steel Castings Handbook, Supplement 5, “General Properties of Steel Castings,” - Ref. No. 6: Wessel, E. T., and Clark, W. T., Jr., “Fracture Prevention Procedure for Heavy Section Components,” Westinghouse scientific paper 70-1E7-FMPWR-P2, January 14, 1970.
8. Westinghouse Electric Company LLC, WCAP-17071-NP, "H*: Alternate Repair Criteria for the Tubesheet Expansion Region in Steam Generators with Hydraulically Expanded Tubes (Model F)," Revision 0, dated April 2009.
9. Holman, J.P., *Heat Transfer*, Fifth Edition, McGraw-Hill, 1981.

Export Control Restrictions

Access to and use of EPRI Intellectual Property is granted with the specific understanding and requirement that responsibility for ensuring full compliance with all applicable U.S. and foreign export laws and regulations is being undertaken by you and your company. This includes an obligation to ensure that any individual receiving access hereunder who is not a U.S. citizen or permanent U.S. resident is permitted access under applicable U.S. and foreign export laws and regulations. In the event you are uncertain whether you or your company may lawfully obtain access to this EPRI Intellectual Property, you acknowledge that it is your obligation to consult with your company's legal counsel to determine whether this access is lawful. Although EPRI may make available on a case-by-case basis an informal assessment of the applicable U.S. export classification for specific EPRI Intellectual Property, you and your company acknowledge that this assessment is solely for informational purposes and not for reliance purposes. You and your company acknowledge that it is still the obligation of you and your company to make your own assessment of the applicable U.S. export classification and ensure compliance accordingly. You and your company understand and acknowledge your obligations to make a prompt report to EPRI and the appropriate authorities regarding any access to or use of EPRI Intellectual Property hereunder that may be in violation of applicable U.S. or foreign export laws or regulations.

The Electric Power Research Institute, Inc. (EPRI, www.epri.com) conducts research and development relating to the generation, delivery and use of electricity for the benefit of the public. An independent, nonprofit organization, EPRI brings together its scientists and engineers as well as experts from academia and industry to help address challenges in electricity, including reliability, efficiency, affordability, health, safety and the environment. EPRI also provides technology, policy and economic analyses to drive long-range research and development planning, and supports research in emerging technologies. EPRI's members represent approximately 90 percent of the electricity generated and delivered in the United States, and international participation extends to more than 30 countries. EPRI's principal offices and laboratories are located in Palo Alto, Calif.; Charlotte, N.C.; Knoxville, Tenn.; and Lenox, Mass.

Together...Shaping the Future of Electricity

Program:

Steam Generator Management Program

3002000411

Electric Power Research Institute
3420 Hillview Avenue, Palo Alto, California 94304-1338 • PO Box 10412, Palo Alto, California 94303-0813 USA
800.313.3774 • 650.855.2121 • askepri@epri.com • www.epri.com